

إزالة الصبغة الزرقاء من مياه المخلفات
بعملية الامتزاز بالفحم المنشط

أطروحة

مقدمة إلى كلية الهندسة جامعة بابل

كجزء من متطلبات نيل درجة ماجستير علوم في

الهندسة المدنية

أعدت من قبل المهندسة

أفراح عبود حسن

٢٠٠٥م

بِسْمِ اللَّهِ الرَّحْمَنِ الرَّحِيمِ

وَمَا أُوتِيتُمْ مِنَ الْعِلْمِ إِلَّا قَلِيلًا

صدق الله العظيم

سورة الإسراء - الآية ٨٦

الملخص

الهدف من العمل التجريبي الحالي هو دراسة إمكانية إزالة الصبغة الزرقاء من المياه الصناعية المتخلفة من الشركة العامة للصناعات النسيجية في الحلة، من خلال عملية الامتزاز بواسطة نظام مستمر الجريان لعمود امتزاز ذو حشوة ثابتة من حبيبات الفحم المنشط.

عدد من التجارب تم تنفيذها لدراسة تأثير متغيرات (معدل الجريان ضمن المدى $(8.33-60) \times 10^{-3}$ م³/دقيقة، تركيز الصبغة الداخل ضمن المدى $(10-50)$ جزء بالمليون، سمك الحشوة ضمن المدى $(10-40) \times 10^{-2}$ م، وحجم حبيبات الفحم المنشط ضمن المدى $(0.6-1.4) \times 10^{-3}$ م) على عمود الامتزاز وتقييم ادائه. وقد وجد ان عملية الامتزاز بالفحم المنشط الحبيبي كانت فعالة في إزالة الصبغة الزرقاء، إذ وصلت نسبة الإزالة إلى 90%.

بيانات حالة التوازن حددت عمليا ولوحظ ان منحنى التوازن الذي يمثل العلاقة بين تركيز التوازن وكمية الامتزاز (كغم مادة ممتزة / كغم كاربون)، هو من النوع المفضل ويتطابق مع معادلتى (لانكمير) و(فرنلش) من خلال الخطأ القياسي ومعامل الترابط للنتائج والتي كانت (نسبة خطأ 7.84، ومعامل الترابط 0.97) لمعادلة لانكمير، و(نسبة الخطأ 4.47، ومعامل الترابط 0.99) لمعادلة فرنلش.

تم دراسة موديل الانحدار الخطي المتعدد بين المتغيرات المستقلة (معدل الجريان (Q)، تركيز الصبغة الداخل (C₀)، سمك الحشوة (Z)، وحجم حبيبات الفحم المنشط (P.S)) والمتغيرات المعتمدة (كمية المادة الممتزة (q)، ووقت الامتزاز (t)) كل على حدة. ان عمل تحقيق لهذه العلاقات وإيجاد معامل الترابط (0.92، 0.94) للعلاقتين على التوالي وضح ان القيم التجريبية مترابطة بشكل جيد مع القيم المحسوبة من معادلة الانحدار الخطي المتعدد.

نظام الدفعات تم تنفيذه للحصول على النفاذية السطحية من خلال مقارنة النتائج العملية والنظرية لنسبة المادة التي تم امتزازها.

تم استخدام موديل رياضي لإيجاد منحنيات التركيز (Breakthrough curves)، وفيه تتركز المقاومة في الطبقة الخارجية للجزيئة إضافة إلى المقاومة المتكونة على السطوح الداخلية لمسامات جزيئة الفحم المنشط، وان عمل تحقيق لهذه العلاقات وإيجاد معامل الترابط والذي كان ضمن المدى $(0.96-0.99)$ وضح ان الموديل يطابق النتائج العملية لهذه الدراسة.



**MY FAITHFUL FAMILY
WHO BURN THE CANDLE AT BOTH
ENDS FOR MY AMBITION**

**THE EYES THAT OBSERVE CLOSELY
THE HEARTS THAT SUPPLICATE FOR
SUCCESS**

CERTIFICATION

We certify that this thesis, entitled "**Removal of blue dye from wastewater by adsorption on activated carbon** " was prepared by "**Afrah Abood Hassan**" under our supervision at Babylon University in partial fulfillment of the requirements for the degree of Master of Science in Civil Engineering.

Signature:

Name :**Prof. Dr. Abass H.
Sulaymon**

Signature:

Name: **Asst. Prof. Dr. Mohammad
A. Muslem Al-Tufaily**

CERTIFICATE

We certify that we have read this thesis, entitled "**Removal of blue dye from wastewater by adsorption on activated carbon**", and as examining committee examined the student "**Afrah Abood Hassan**" in its contents and in what is connected with it, and that in our opinion it meets the standard of a thesis for the degree of Master of Science in Civil Engineering.

Signature:
Name: Asst. Prof. Dr. Malik M. Mohammad
(Member)

Date: / / ٢٠٢٠

Signature:
Name: Asst. Prof. Dr. Jabar H. Al-Baithani
(Member)

Date: / / ٢٠٢٠

Signature:
Name: Prof. Dr. Raza H. Al-Suhaili
(Chairman)

Date: / / ٢٠٢٠

Signature:
Name: Prof. Dr. Abass H. Sulaymon
(Supervisor)

Date: / / ٢٠٢٠

Signature:
Name: Asst. Prof. Dr. Mohammad A. M. Al-Tufaily
(Supervisor)

Date: / / ٢٠٢٠

Approval of the Civil Engineering Department
Head of the Civil Engineering Department

Signature:
Name: Asst. Prof. Dr. Ammar Y. Ali
Date: / / ٢٠٢٠

Approval of the Deanery of the College of Engineering
Dean of the College of Engineering

Signature:
Name: Asst. Prof. Dr. Haroun A. K. Shahad
Dean of the College of Engineering
University of Babylon
Date: / / ٢٠٢٠

ACKNOWLEDGMENTS

Praise be to **ALLAH HIS MAJESTY** for this work has been completed under His benediction.

I would like to express my sincere gratitude and respect to my supervisors **Prof. Dr. Abass H. Sulaymon and Asst. Prof. Dr. Mohammad A. Muslem Al-Tufaily** for their encouragement and continuous guidance through this work.

I wish to express my gratefulness to Mr. Alaa Hamza Daham a chief of the finishing department, and Mr. Abd Al-Hussein Shakir a chief of the water Purification department in textile company for their assistance throughout this work.

My respectful regards to the head **Dr. Ammar Y. Ali** and staff of Civil Engineering Department For their helpfulness.

I wish to express my gratefulness to the staff of fluid, sanitary, Soil and computer labs for their assistance throughout this work.

I am very indebted to Mr.Waleed M. Abood for all the facilities he rendered me.

Finally, I wish to express my deepest respect and sincere appreciation to my family especially my mother and father for their supports and helpfulness during my study.

Many others are not mentioned explicitly here, their efforts are equally appreciated.

REMOVAL OF BLUE DYE FROM WASTEWATER BY ADSORPTION ON ACTIVATED CARBON

A thesis

**Submitted to the College of Engineering
of the University of Babylon in partial
fulfillment of the requirements
for the degree of Master
of Science in Civil
Engineering**

By

AFRAH ABOOD HASSAN

٢٠٠٥

ABSTRACT

This work was conducted to study the blue dye removal from textile company wastewater by the adsorption process using continuous system (fixed-activated carbon bed).

Experiments were carried out to study the effect of various conditions [flow rate Q within the range of $(8.33-60) \times 10^{-3}$ m³/min, concentration C_0 within the range of $(10-50)$ ppm, bed depth Z within the range of $(1-5) \times 10^{-2}$ m and particle size of activated carbon P.S within the range of $(0.7-1.5) \times 10^{-3}$ m], on the performance of fixed bed. Adsorption through granular activated carbon was found to be very effective for the removal of the blue dye, where the percent dye removal was 90%.

The equilibrium data were determined experimentally and the equilibrium isotherm was found to be of a favorable type and fit well by Langmuir and Freundlich isotherms, while experimental and theoretical results were compared by estimating the standard error and correlation coefficient for the results with the value of (St. Err = 2.57, and $R=0.99$) for Langmuir isotherm and (St. Err. = 7.82, and $R=0.97$) for Freundlich isotherm.

The study was developed a multiple linear regression model between the independent variables (Q , C_0 , Z , P.S) and the dependent variables (Time t , Amount of adsorbate q) separately, the verification and the correlation coefficient (R) (0.92 , and 0.90) for these correlation respectively, illustrate that the experimental data correlated well with the modeling data.

Batch process was carried out to obtain the surface diffusivity by comparing the experimental and theoretical results of the fractional uptake.

The mathematical model for external diffusion combined with surface diffusion resistance was used to predict the breakthrough curves. The verification and the correlation coefficient (R) within the range of $(0.962-0.992)$ illustrate that this model was in a good agreement with the experimental data.

Contents

SECTION	ADDRESS	PAGES
	Abstract	I
	Contents	II
	List of tables	IV
	List of figures	IV
	Nomenclature	VII
CH-1	INTRODUCTION	
1.1	Introduction	1
1.2	Aim of the study	2
CH-2	LITERATURE REVIEW AND THEORETICAL CONCEPT	
2.1	Historical review	4
2.2	Textile wastes	4
2.3	Adsorption	5
2.4	Adsorption isotherm	6
2.5	Adsorption equilibrium relationships	8
2.6	Adsorption in fixed bed	10
2.7	Batch processes	12
2.8	Selection of experimental conditions	12
2.8.1	Effect of particle size of adsorbent	12
2.8.2	Effect of influent concentration	13
2.8.3	Effect of flow rate	14
2.8.4	Effect of bed depth	15
2.9	Rate-limiting step	15
2.10	Kinetic of adsorption	18
2.10.1	Mathematical model for batch adsorber	20
2.10.2	Measurement of surface diffusivity	21
2.10.3	Mathematical model for fixed bed adsorber	23
CH-3	EXPERIMENTAL WORK	
3.1	Material	25
3.1.1	Adsorbate	25
3.1.2	Adsorbent	26
3.1.3	Preparation of Samples	28

३.२	Experimental arrangements	२८
३.२.१	Equilibrium isotherm experiment	२८
३.२.२	Column system (continuous system)	२९
३.२.२.१	Equipment	२९
३.२.२.२	Procedure	३०
३.२.३	Batch system	३१
३.२.३.१	Equipment	३१
३.२.३.२	Procedure	३२
३.३	Analysis system	३२
३.३.१	Dye concentration	३२
३.३.२	Determine of other pollutants	३३
CH-६	RESULTS AND DISCUSSIONS	
६.१	Langmuir and Freundlich isotherm equations	३०
६.२	Column experiments	३७
६.२.१	Effect of flow rate	३७
६.२.२	Effect of influent concentration	६१
६.२.३	Effect of bed depth	६६
६.२.६	Effect of particle size	६९
६.३	Development of multiple linear regression models	०३
६.६	Predicting the isothermal adsorption breakthrough curves	००
CH-०	CONCLUSIONS AND RECOMMENDATIONS	
०.१	Conclusions	६१
०.२	Recommendations	६२
	References	
	Appendix A	
	Appendix B	
	Appendix C	
	Appendix D	
	Appendix E	
	Appendix F	

List of tables

NO.	ADDRESS OF TABLE	PAGE
CH-۳	CHAPTER THREE	
۳.۱	Properties of activated carbon used in this research	۲۷
۳.۲	Column system data	۳۱
CH-۴	CHAPTER FOUR	
۴.۱	Langmuir and Freundlich equations constants	۳۷
	Appendix D	
(D-۱)	Physical properties and parameters used in the mathematical model	

List of Figures

NO.	ADDRESS OF FIGURE	PAGE
	CHAPTER TWO	
۲.۱	Adsorption isotherm for reactive blue dye on activated carbon	۷
۲.۲	Types of sorption separations	۷
۲.۳	Schematic representation of the movement of the adsorption zone and the resulting breakthrough curve	۱۱
۲.۴	Modes of uptake within the adsorbent particle	۱۵
۲.۵	Schematic illustration of the experimental batch process	۱۹
CH-۳	CHAPTER THREE	
۳.۱	Molecular structure of reactive blue dye	۲۵
۳.۲	Exaggerated representation surface and pores of adsorbent	۲۸
۳.۳	A schematic representation of experimental equipment	۳۰
۳.۴	Photo of Experimental pilot plant	۳۴

CH-ε	CHAPTER FOUR	
ε.1	Parameters for the Langmuir's equation	30
ε.2	Parameters for the Freundlich's equation	36
ε.3	Experimental and theoretical data were obtained from the Langmuir's and Freundlich's equations for the adsorption ratio	36
ε.4	Breakthrough curves of isotherm adsorption for different wastewater's flow rate	38
ε.5	Adsorption ratio curves for different wastewater's flow rates	38
ε.6	Effect of the wastewater's flow rate on the adsorption capacity of activated carbon	40
ε.7	Effect of the wastewater's flow rate on the rate of mass transfer	40
ε.8	Breakthrough curves of isotherm adsorption for different influent concentration of dye	42
ε.9	Adsorption ratio curves at different influent concentration of dye	42
ε.10	Effect of different influent concentration on the adsorption capacity of activated carbon	43
ε.11	Effect of different influent concentration on the rate of mass transfer	44
ε.12	Breakthrough curves of isotherm adsorption for different bed depth of activated carbon	40
ε.13	Adsorption ratio curves at different bed depth	46
ε.14	Effect of different bed depth of activated carbon on the adsorption capacity of activated carbon	47
ε.15	Effect of different bed depth of activated carbon on the rate of mass transfer	48
ε.16	Breakthrough curve of isotherm adsorption for industrial wastewater	49
ε.17	Breakthrough curves of isotherm adsorption for different particle size of activated carbon	50
ε.18	Adsorption ratio curves at different particle size of activated carbon	51
ε.19	Effect of different particle size on the adsorption capacity of activated carbon	51
ε.20	Effect of different particle size of activated carbon on the rate of mass transfer	52
ε.21	Verification curve for regression equation	54
ε.22	Verification curve for regression equation	54

ξ.23	Experimental and predicted breakthrough curves for isothermal adsorption at bed depth ($1.1 \cdot 10^{-2}$)m	06
ξ.24	Experimental and predicted breakthrough curves for isothermal adsorption at bed depth ($3.1 \cdot 10^{-2}$)m	06
ξ.25	Experimental and predicted breakthrough curves for isothermal adsorption at concentration (10 ppm)	07
ξ.26	Experimental and predicted breakthrough curves for isothermal adsorption at concentration (30 ppm)	07
ξ.27	Experimental and predicted breakthrough curves for isothermal adsorption at flow rate ($33.33 \cdot 10^{-6}$)m ³ /min	08
ξ.28	Verification curve of $Z=1.1 \cdot 10^{-2}$ (m)	08
ξ.29	Verification curve of $Z=3.1 \cdot 10^{-2}$ (m)	09
ξ.30	Verification curve of $C=10$ (ppm)	09
ξ.31	Verification curve of $C=30$ (ppm)	10
ξ.32	Verification curve of $Q=33.33 \cdot 10^{-6}$ (m ³ /min)	10
APPENDIX C		
C-1	Experimental (w_0/w_∞) for batch isotherm system at ($C_0=30$ ppm) and speed (100 rpm)	
C-2	Plot of (w_0/w_∞) vs. (TH) for determination of surface diffusivity ($TH=D_s t/R^2$) at $\lambda > 1$	
C-3	Plot of (TH) vs. (time) at average value of (D_s)	

Nomenclature

Symbol	Definition	Unit
b	Langmuir equation parameter	(m ³ /kg)
C	Dye concentration at given time	(ppm)
C _o	Initial concentration of dye	(ppm)
C _e	Dye concentration at equilibrium	(ppm)
C _{ef}	Effluent dye concentration	(ppm)
C _{Fo}	Initial fluid phase concentration	(mol/L)
d	Particle diameter	(m)
D	Molecular diffusivity	(m ² /s)
D _p	Pore diffusivity	(m ² /s)
D _s	Surface diffusivity	(m ² /s)
e	Void fraction of bed	
e _p	Porosity of particle	
K	Freundlich equilibrium parameter	(kg/kg)
K _e	Sorption equilibrium constant	
K _m	Mass transfer coefficient	(m/s)
m	Mass of activated carbon	(kg)
M _B	Molecular weight of solvent	(kg/kg mol)
M _t	Adsorbate uptake at given time	(m mol/cm ³)
MTZ	Mass transfer zone	
M _t /M _∞	Fractional up take	
1/n	Freundlich equation parameter	(m ³ /kg)
N _σ	Total uptake at equilibrium	(m mol/cm ³)
q	Adsorption ratio at given time	(kg/kg of carbon)
q _e	Adsorption ratio at equilibrium	(kg/kg of carbon)
q _r	Mass of transfer rate	(kg/kg/s)
q _R	Concentration of adsorbate at the particle surface	(kg/kg of carbon)
q _n	Constants of theoretical model of batch process	
Q	Flow rate	(m ³ /min)
\bar{Q}	Langmuir equation parameter	(kg/kg)
r	Radial distance from center of particle	(m)

R	Particle radius	(m)
R_e	Reynolds No.	
S_C	Schmidt No.	
t	Time	(min)
T	Temperature	(k)
TH	Through put value dimensionless	
V	Linear velocity	(m/s)
V_L	Volume of liquid in batch process	(m ³)
V_p	Volume of adsorbent	(m ³)
(w_o/w_∞)	Fractional up take	
X	Mass of adsorbate	(kg)
Z	Bed depth of adsorbent	(m)

Greek symbols:

α : Effective area for mass transfer across the fluid film per unit volume of bed. (m²/m³)

η : $e/(1-e)$

ρ : Fluid density. (kg/m³)

ρ_b : Bulk density of bed. (kg/m³)

μ : Viscosity. (kg/m.s)

ν : Kinematics viscosity. (m²/s)

λ, θ : Effective volume ratio

APPENDIX A

CALIBRATION CURVE

Prediction of Absorbency – Concentration Relationship:

The most application method for the measurement of concentration of dye is the absorbency measurement. For this purpose the relation between the concentration of dye solution and absorbency was determined.

Fig (A-1) below shows the plot of absorbency of reactive blue dye versus the concentration in (ppm) at (679 nm).

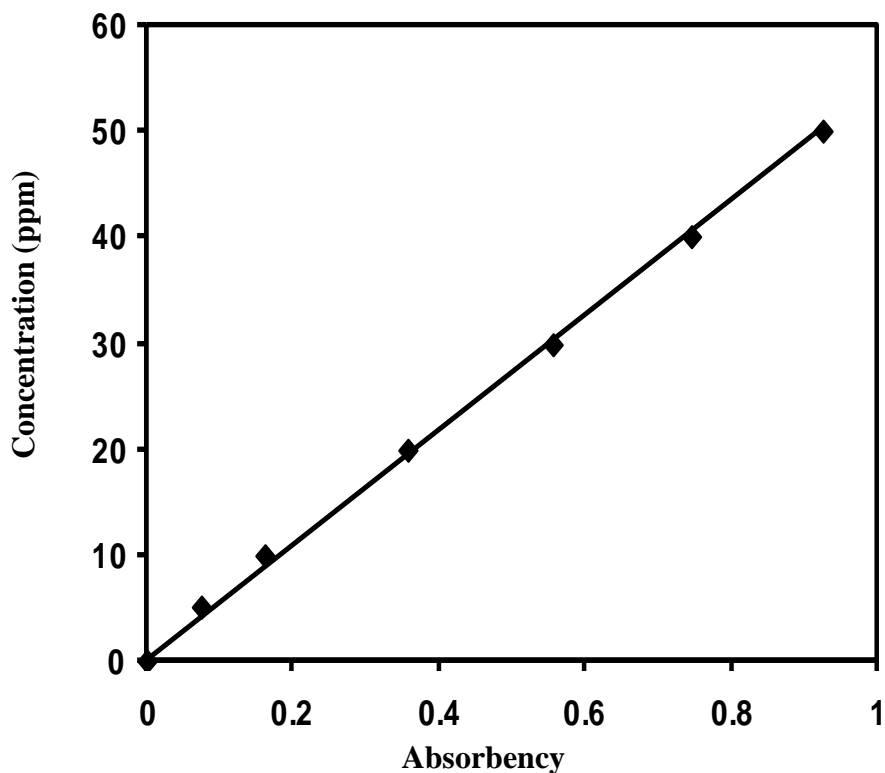
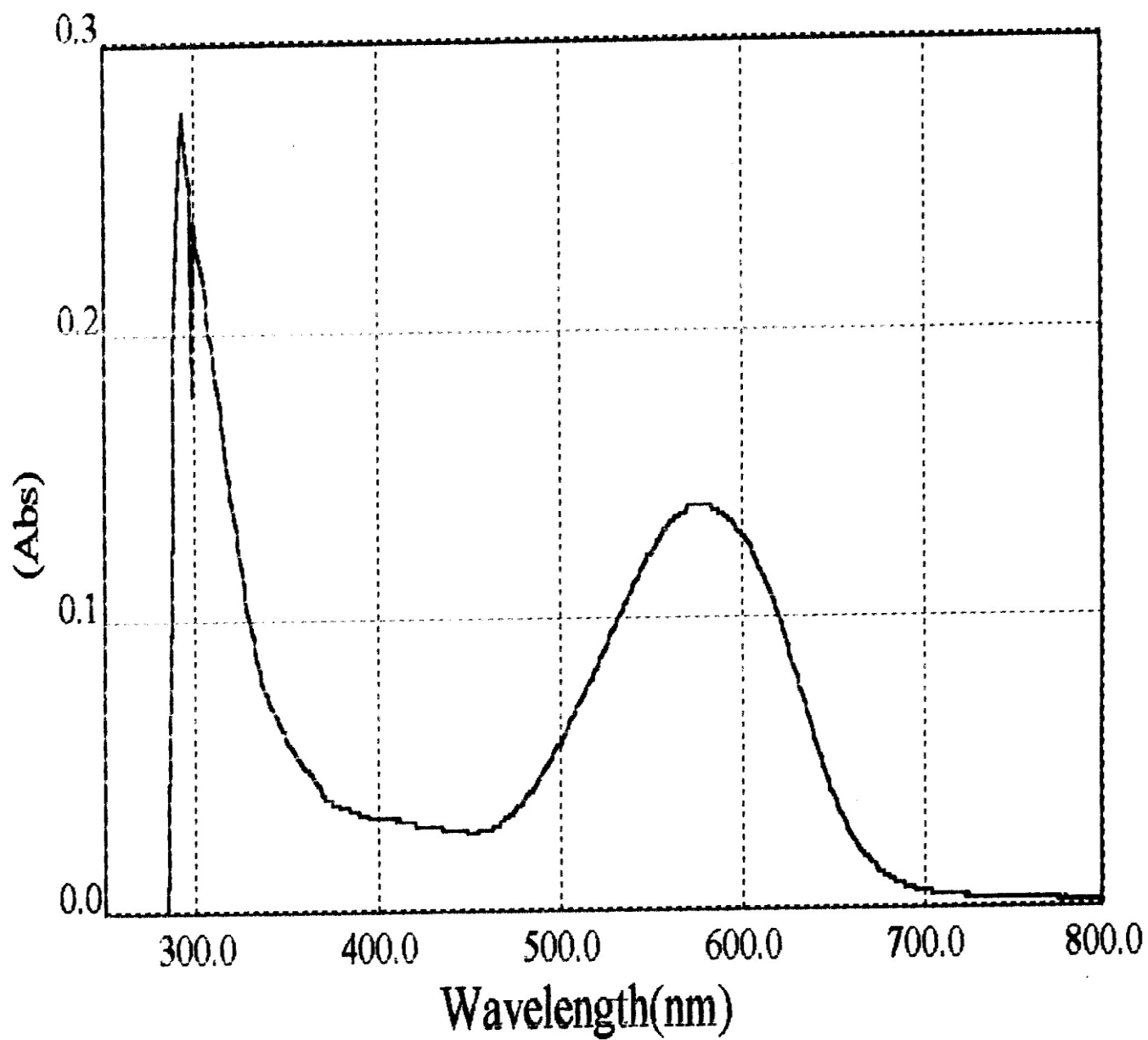


Fig (A-1): Relation between concentration and absorbency for reactive blue dye (in water)

This figure has the following predicted equation:

$$C = 0.923 * ABS + 1.32$$



APPENDIX B

Sample of Calculations

1. The amount of adsorbed dye:

Adsorption ratio (q) has been calculated by, the quantity of adsorbed dye per unit mass of activated carbon

$$q = [(C_0 - C)/m] * Q * t \quad (\text{kg of solute / kg of carbon})$$

Accumulative calculations were made to obtain value of (q) after a given time of adsorption.

For example the condition of experiment [No. (1), table (3-3)].

$$C_0 = 3 \text{ ppm}$$

$$m = 0.09 \text{ kg of carbon}$$

$$Q = 6.1 \times 10^{-3} \text{ m}^3/\text{min}$$

The effluent concentration after every (10 min) was tabulated in table (E-2) Appendix (E).

The value of (q) after (10 min) was:

$$[(3 - 2.5) * 10^{-3} / 0.09] * 6.1 \times 10^{-3} * 10 = 3.33 \times 10^{-4} \text{ kg/kg of carbon}$$

The value of (q) after (30 min) will be:

$$[(3 - 2.5) * 10^{-3} / 0.09] * 6.1 \times 10^{-3} * 30 + 3.33 \times 10^{-4} = 7.9 \times 10^{-4} \text{ kg/kg of carbon}$$

The adsorption capacity:

This represents the ability of carbon for adsorbing the adsorbate per unit mass of carbon in the equilibrium and represent the last value of (q) in experiment of continuous system, i.e. table (E-2) in Appendix E for flow rate ($6.1 \times 10^{-3} \text{ m}^3/\text{min}$) the value is (39.32×10^{-4}) kg/kg of carbon.

The rate of mass transfer [kg/kg/s]:

This is represented by the slopes of the linear portion of the adsorption quantity curves (q vs. time).⁽¹⁴⁾

The linear portion will represent the mass transfer due to diffusion and the rest of the curve represents the mass transfer caused by the intraparticle transport (since the diffusion process is faster than the intraparticle transport it will occur rapidly).⁽¹⁵⁾

Appendix C

Measurement of surface diffusivity (D_s)

Measurement of surface diffusivity (D_s):

The results of (w_o/w_∞) from experimental batch process were against time. Fig (C-1)

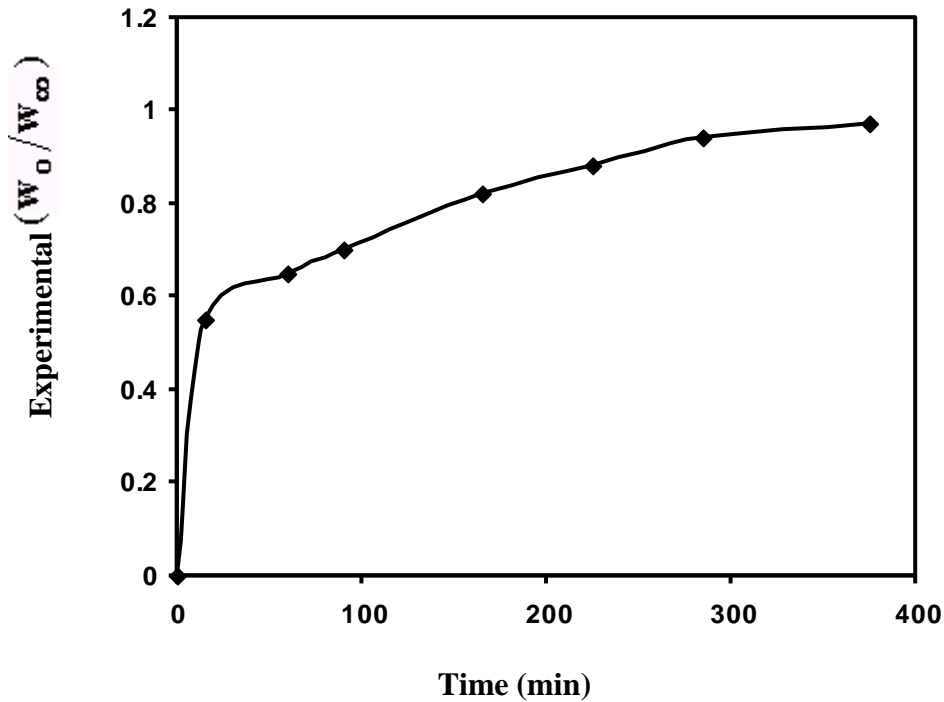


Fig (C-1): Experimental (w_o/w_∞) for batch isotherm system at $(C_o = 3 \text{ ppm})$ and speed (900 rpm)

The theoretical values of (w_o/w_∞) were obtained from equation (C-1) for granular shape of activated carbon:

$$w_o/w_\infty = 1 - \sum_{n=1}^{\infty} \frac{6\lambda(1+\lambda)}{9\lambda(1+\lambda) + \lambda^2 q_n^2} \exp[-q_n^2 TH] \quad \dots\dots(C-1)$$

Where values of (q_n) were obtained from table (1). ⁽¹⁾

For $\lambda \geq 10$, $\implies q_1 = 3.142$ $q_2 = 6.284$

Fig (C-2) shows the plotting of the theoretical value of (w_0/w_∞) against (TH), which were obtained from above equation (C-1).

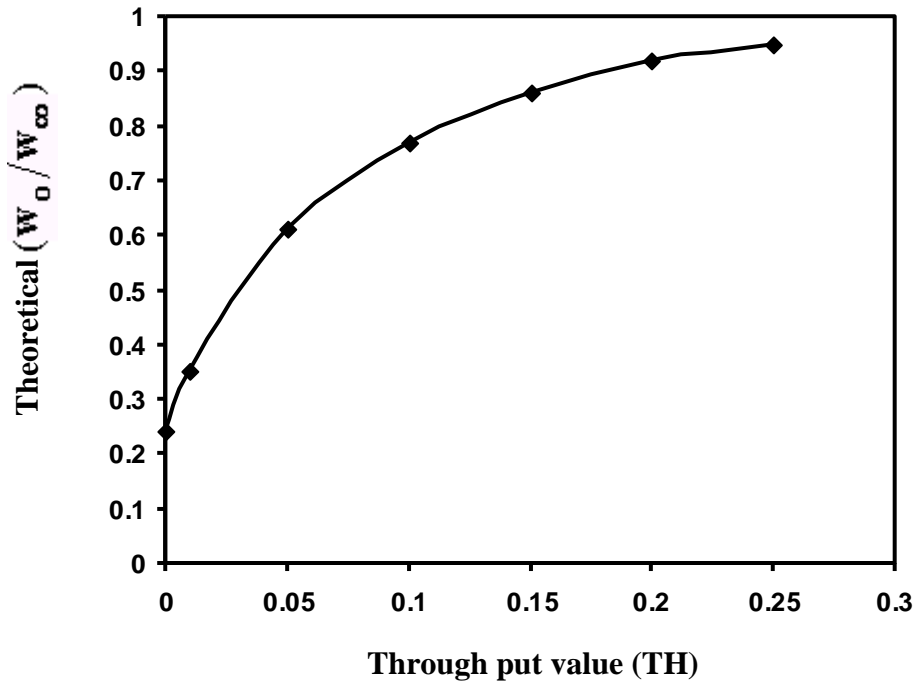


Fig (C-2): Plot of (w_0/w_∞) Vs. (TH) for determination of surface diffusivity ($TH = D_s t/R^2$) at $(\lambda > 10)$

The values of time (i.e. determination of surface diffusivity) were obtained from theoretical values of (w_0/w_∞) and Fig (C-1).

The values of (D_s) were obtained from the following relation ($D_s = TH R^2/t$), the values of (TH) from Fig (C-2) and known particle radius, therefor average value of (D_s) a linear relation between (TH) and time was plotted as Fig (C-3).

The experimental result were tabulated in table (E-5), Appendix E.

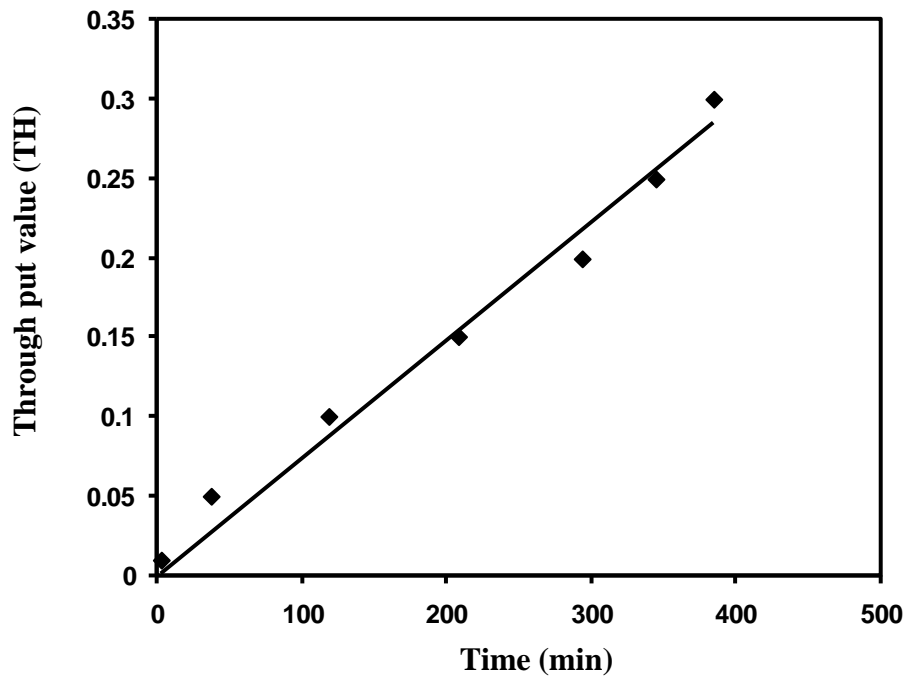


Fig (C- r): Plot of (TH) vs. (Time) at average value of (D_s)

APPENDIX D

Mathematical model used for the prediction of isothermal adsorption breakthrough curves

Model employed the external diffusion combined with surface diffusion:
(D-1)

When surface diffusion is the main internal mass transfer process, the diffusion mechanism can be expressed as. (D-1,1v)

$$\frac{\partial q}{\partial t} = \frac{D_s}{r^2} \frac{\partial}{\partial r} \left(r^2 \frac{\partial q}{\partial r} \right) \dots\dots\dots(D-1)$$

The average intraparticle concentration was

$$\bar{q} = \frac{3}{r^2} \int_0^R q r^2 dr \dots\dots\dots(D-2)$$

The rate of change of (\bar{q}) was obtained upon differentiation of equation (D-2).

$$\frac{\partial \bar{q}}{\partial t} = \frac{3}{R^3} \int_0^R \left(\frac{\partial q}{\partial t} \right) r^2 dr \dots\dots\dots(D-3)$$

Substituting equation (D-1) into (D-3)

$$\frac{\partial \bar{q}}{\partial t} \frac{3}{R^3} \int_0^R D_s \frac{\partial}{\partial r} \left(r^2 \frac{\partial q}{\partial r} \right) dr \dots\dots\dots(D-4)$$

$$= \frac{3 D_s}{R} \left(\frac{\partial q}{\partial r} \right) \dots\dots\dots(D-5)$$

The equation of continuity of the mobile fluid phase was expressed by:

$$v \frac{\partial c}{\partial z} + \frac{\partial c}{\partial t} = -\left(\frac{\partial \bar{q}}{\partial t}\right) / \eta \quad \dots\dots\dots(D-7)$$

Where $\eta = e/(1-e)$

The usual assumptions were made in connection with equation (D-7):

- 1- The velocity and concentration of mobile fluid phase were independent of radial position at any cross section of the bed.
- 2- Axial diffusion was negligible.
- 3- Temperature and pressure were uniform in the bed.

Assume:

$$X = z/(\eta v) \quad \dots\dots\dots(D-8)$$

$$\Theta = t - z/v \quad \dots\dots\dots(D-9)$$

Equation (D-7) was simplified when expressed in terms of the new variables.

$$\frac{\partial c}{\partial X} = -\frac{\partial \bar{q}}{\partial \Theta} \quad \dots\dots\dots(D-10)$$

The equilibrium at the surface between fluid and solid was taken to be linear. ⁽¹⁰⁾

$$q_R = k_e C_{eq} \quad \dots\dots\dots(D-11)$$

The resistance at the surface was controlled at the film transfer coefficient, so that

$$D_s \left. \frac{\partial q}{\partial r} \right|_{r=R} = K_m (C - C_{eq}) = K_m (C - q_R / K_e) \quad \dots\dots\dots(D-12)$$

Combining equations (D-10) and (D-12)

$$\frac{\partial \bar{q}}{\partial \Theta} = \frac{3k_m}{R} (C - q_R / k_e) \quad \dots\dots\dots(D-13)$$

Equations (D-9), (D-11) and (D-12) make up a set of simultaneous equations for (C) and (q).

Eliminate (q) from the equations to obtain a partial differential equation for (C) only upon simulating (q) with a parabola as in equation (D-13).

$$\mathbf{q} = \mathbf{a}_0 + \mathbf{a}_2 \mathbf{r}^2 \quad \dots\dots\dots(\text{D-13})$$

Where \mathbf{a}_0 and \mathbf{a}_2 were functions of time (t).

$$\mathbf{q}_R = \mathbf{a}_0 + \mathbf{a}_2 \mathbf{R}^2 \quad \dots\dots\dots(\text{D-14})$$

$$\left. \frac{\partial \mathbf{q}}{\partial \mathbf{r}} \right|_{\mathbf{r}=\mathbf{R}} = 2\mathbf{a}_2 \mathbf{R} \quad \dots\dots\dots(\text{D-15})$$

$$\bar{\mathbf{q}} = \mathbf{a}_0 + (3/5)\mathbf{a}_2 \mathbf{R}^2 \quad \dots\dots\dots(\text{D-16})$$

Combining equations (D-11), (D-14), (D-15) and (D-16) to get

$$\bar{\mathbf{q}} = \left[1 + \frac{\mathbf{R} \mathbf{k}_m}{5 \mathbf{D}_s \mathbf{k}_e} \right] \mathbf{q}_R - \frac{\mathbf{R} \mathbf{k}_m}{5 \mathbf{D}_s} \mathbf{C} \quad \dots\dots\dots(\text{D-17})$$

Differentiation of equation (D-17) gives

$$\frac{\partial \bar{\mathbf{q}}}{\partial \Theta} = \left[1 + \frac{\mathbf{R} \mathbf{k}_m}{5 \mathbf{D}_s \mathbf{k}_e} \right] \frac{\partial \mathbf{q}_R}{\partial \Theta} - \frac{\mathbf{R} \mathbf{k}_m}{5 \mathbf{D}_s} \frac{\partial \mathbf{c}}{\partial \Theta} \quad \dots\dots\dots(\text{D-18})$$

To eliminate $(\partial \mathbf{q}_R / \partial \Theta)$ from equation (D-18), substituting equation (D-9) into (D-17) and differential to obtain:

$$\frac{\partial q_R}{\partial \Theta} = \frac{k_e R}{3k_m} \frac{\partial^2 C}{\partial X \partial \Theta} + k_e \frac{\partial C}{\partial \Theta} \quad \dots\dots\dots(D-19)$$

Substituting equation (D-19) and (D-18)

$$\frac{\partial C}{\partial X} = -k \frac{\partial C}{\partial \Theta} - E \frac{\partial^2 C}{\partial X \partial \Theta} \quad \dots\dots\dots(D-20)$$

Where:

$$E = R \left[\frac{k_e}{3k_m} + \frac{R}{15D_s} \right] \quad \dots\dots\dots(D-21)$$

In equation (D-20), (q) was eliminated and equation for (C) only was obtained. The concentration was more conveniently expressed in a reduced form.

$U = \frac{C}{C_0}$ and equation (D-20) becomes:

$$\frac{\partial u}{\partial X} = -k_e \frac{\partial u}{\partial \Theta} - E \frac{\partial^2 u}{\partial X \partial \Theta} \quad \dots\dots\dots(D-22)$$

Equation (D-22) was solved with the following initial and boundary conditions:

$$\begin{aligned} U &= 0 & \text{at } \Theta &\leq 0 & \text{and all } x \\ U &= 1 & \text{at } \Theta &> 0 & \text{and } x=0 \end{aligned}$$

Equation (D-22) was solved by Laplace transformation, the solution was given below:

$$U_N = e^{\oplus + x} \left[1 + \sum_{i=1}^N \left[\prod_{k=1}^i \frac{\oplus}{k} \right] \left[1 + \sum_{j=1}^i \prod_{m=1}^j \frac{X}{m} \right] \right] \dots\dots\dots(D-23)$$

Where: $\oplus = -\ominus / E$ \dots\dots\dots(D-24)

$$x = -k_e X / E \quad \dots\dots\dots(D-25)$$

An error of not more than 0.1% was incurred with N=8.

Equation (D-23) was the working formula expressing concentration of the adsorbate in the fluid as a function of time and axial distance.

Mass transfer coefficient (k_m) was computed from the general correlation for mass transfer. ^(26,28)

$$\frac{k_m d_p}{D} = 2 + 1.45 Re^{1/2} Sc^{1/3} \quad \dots\dots\dots(D-26)$$

Where: $Re = \frac{\rho u d}{\mu}$ \dots\dots\dots(D-27)

$$Sc = \nu / D \quad \dots\dots\dots(D-28)$$

Evaluation of this correlation requires an estimate of molecular diffusivity (D). Molecular diffusivity can be estimated from the Wilke-Chang correlation. ⁽²⁸⁾

$$D = 7.4 \times 10^{-8} \left[\frac{(\phi M_B)^{1/2} T}{\mu_B V_A^{0.6}} \right] \quad \dots\dots\dots(D-29)$$

Where ϕ = association parameter of solvent (for water = 2.6)

V_A = molal volume of the solute at its normal boiling point (cm^3/mol)

Surface diffusivity (D_s) was obtained from comparing experimental with theoretical data as illustrated in Appendix (C).

(K_e) is the adsorption equilibrium constant for linear isotherm. (23) It was obtained from the slope of the linear segment in Fig (2-1).

Table (D-1) shows the parameters used in the mathematical model. Appendix-F shows a computer program for the solution of equation (D-23).

Table (D-1): Physical properties and parameters used in the mathematical model

Parameter	The value	Unit
d_p	1.1×10^{-3}	(m)
e	0.40	-
D	2.74×10^{-9}	(m^2/s)
D_s	0.70×10^{-12}	(m^2/s)
K_m	0.136×10^{-4}	(m/s)
K_e	7.42	-
μ	0.7042	(kg/m.s)

APPENDIX E

Table (E-1): Experimental and theoretical equilibrium isotherm data

Equilibrium Concentration (ppm)	Experimental isotherm data $q_e(\text{kg/kg})^{*10^{-4}}$	Langmuir isotherm data $q_e(\text{kg/kg})^{*10^{-4}}$	Freundlich isotherm data $q_e(\text{kg/kg})^{*10^{-4}}$
20	100	101	107
10	80	70	68
5	50	50	44
3	27	34	32
1.3	19	17	19
1	10	13	16

Table (E-4): Break through and adsorption quantity data for different bed depth
 Where: C (ppm) and q (kg/kg) *10⁻⁴

Time (min)	Bed depth (4.0*10 ⁻¹ m)		Bed depth (3.0*10 ⁻¹ m)		Bed depth (2.0*10 ⁻¹ m)		Bed depth (1.0*10 ⁻¹ m)	
	C	q	C	q	C	q	C	q
10	0	2.37	1.6	2.99	3	4.03	14.8	4.8
30	1.0	4.72	2.3	5.91	5.8	7.80	15.7	9.32
40	1.6	6.86	3.2	8.73	7.1	11.47	16.8	13.49
60	1.7	9.09	4	11.47	8.9	14.8	17.2	17.03
70	1.8	11.32	4.7	14.13	10.6	17.86	19.3	20.91
90	2	13.53	5.6	16.7	12.4	20.64	20.4	23.94
100	2.2	15.72	6.4	19.18	15.1	22.99	21.6	26.09
120	2.4	17.89	7.1	21.09	15.4	25.3	22.3	29.02
130	2.6	20.00	8.0	23.80	16.0	27.43	24.0	30.76
150	2.8	22.19	10	25.96	17.3	29.44	25.7	32.12
160	3.1	24.31	11.8	27.88	17.9	31.30	26.3	33.29
180	3.4	26.41	12.0	29.72	18.4	33.18	26.8	34.29
190	3.7	28.48	13.3	31.48	19.2	34.89	27.2	35.178
210	4	30.00	13.7	33.2	19.8	36.00	27.8	35.87
220	4.4	32.02	14.2	34.86	20.6	37.98	28.3	36.41
240	4.8	34.01	14.9	36.40	21.0	39.32	28.7	36.82
250	5.3	36.46	15.3	38	22.7	40.47	29	37.136
270	5.8	38.37	15.8	39.49	23.6	41.48	29.0	37.29
280	6.3	40.24	16.0	40.91	24.3	42.38	30	
300	6.9	42.06	16.7	42.31	24.9	43.19		
310	7.0	43.84	17.2	43.66	25.7	43.87		
330	8.2	45.56	17.4	44.99	27.0	44.27		
340	9	47.22	18	46.20	28.4	44.52		
360	10	48.79	18.8	47.43	30			
370	11	50.29	19.0	48.04				
390	12.1	51.7	20.3	49.06				
400	13.4	53.01	21.1	50.00				
420	14.7	54.23	21.8	51.36				
430	16	55.34	23	52.1				
450	17.3	56.34	24.1	52.72				
460	18.9	57.22	25.0	53.19				
480	20.9	57.94	26.4	53.57				
490	23	58.49	27.2	53.86				
510	25.2	58.87	27.9	54.08				
520	26.1	59.18	28.4	54.20				
540	26.9	59.42	29.2	54.33				
550	27.6	59.61	30					
570	28.1	59.76						
580	28.5	59.88						
600	28.8	59.97						
610	29.4	60.00						
630	30							

Table (E- 6): Break through and adsorption data for different particle size.
 Where: C (ppm) and q (kg/kg)*10⁻⁴

Time	Particle size(1.4*10 ⁻³ m)		Particle size(1.18*10 ⁻³ m)		Particle size(0.7*10 ⁻³ m)	
	C	q	C	q	C	q
10	6.7	3.68	0	3.90	1.8	4.40
30	6.8	7.34	0.1	7.88	2.1	8.80
40	6.94	10.98	0.2	11.79	2.4	13.2
60	7.09	14.09	0.6	10.64	2.8	17.0
70	7.26	18.18	6	19.4	3.2	21.7
90	7.76	21.69	6.4	23.13	3.7	20.9
100	8.36	20.11	6.9	26.78	4.2	29.97
120	9.3	28.38	7.4	30.30	4.8	33.90
130	10.4	31.47	8	33.82	0.0	37.82
150	12.10	34.29	8.7	37.18	6.2	41.08
160	13.90	37.82	9.4	40.43	6.9	40.23
180	16.10	39	10.2	43.06	7.8	48.74
190	18.30	40.84	11	46.06	9.1	02.04
210	20.70	42.3	12.0	49.32	11.2	00
220	23.40	43.33	13.7	01.89	12.0	07.76
240	24.70	44.16	10.9	04.12	14.3	6.24
250	20.60	44.80	19.8	00.73	17.8	62.17
270	26.70	40.36	21.7	07.04	19.4	63.84
280	27.40	40.76	22.6	08.21	21.1	60.20
300	28.00	46.07	26.1	08.83	22.4	66.40
310	28.70	46.27	26.8	09.33	23.6	67.46
330	30		27.0	09.72	24.3	68.36
340			28.3	09.99	20.7	69.04
360			30		26.2	69.64
370					27.0	70.03
390					28.1	70.33
400					28.8	70.02
420					30	
430						
450						
460						
480						
490						
510						
520						
540						
550						
570						
580						
600						
610						
630						

Table (E-٦): Data of investigation of other pollutants

Time (min)	CL(mg/L)	SO₄(mg/L)	T.H(mg/L)	Ca(mg/L)	Mg(mg/L)
١٥	٢٩٩.٩	٥٧٤.٥	٢٤٤	٢٢٠	٢٤
٣٠	٢٨٩.٩	٢٣٥	١٩٢	١٧٨	١٤
٤٥	٢٩٥.٩	٣٥٠.٣	٢٢٨	١٩٦	٣٢
٦٠	٢٩٣.٨	٤٢٠.٧	٢٢٠	١٨٧	٣٣
٧٥	٢٩٥.٩	٤٨٠.٣	٢٢٦	١٩٥	٣١
٩٠	٢٩٩.٥	٥٣٠	٢٣٩	٢١٦	٢٣
١٠٥	٢٩٩.٩	٤٩٢.٦	٢٤٠	٢١٩	٢١
١٢٠	٢٩٧.٨	٤٨٠.٣	٢٣٧	٢١٤	٢٣

Table (E-7): Experimental and theoretical results of surface diffusivity calculation

Time (min)	Experimental fractional up take (w_0/w_∞)	Theoretical fractional up take (w_0/w_∞)	Through put value
0	0	0.24	0
10	0.50	0.30	0.1
60	0.60	0.61	0.50
90	0.7	0.77	0.1
160	0.82	0.86	0.10
220	0.88	0.92	0.2
280	0.94	0.90	0.20
370	0.97	0.97	0.3

APPENDIX F

Computer program for the mathematical model

```
1. REM *** Program for calculating the breakthrough curves for the
   mathematical model ***
2. N=0.
3. FOR TH=-0.6 TO -2.89 STEP (-0.301)
4. X=-0.70
5. S1=EXP (TH+X)
6. S=.
7. FOR I=1 TO N
8. P1=1
9. FOR K=1 TO I
10. P1=P1*ABS (TH)/K
11. NEXT K
12. S2=.
13. FOR J=1 TO I
14. P2=1
15. FOR M=1 TO J
16. P2=P2*ABS (X)/M
17. NEXT M
18. S2=S2+P2
19. NEXT J
20. S2=S2+1
21. S=S+P1*S2
22. NEXT I
23. UN=S1*(S+1)
24. PRINT TH, UN
25. NEXT TH
26. END
```

CHAPTER FIVE CONCLUSIONS AND RECOMMENDATIONS

5.1 Conclusions:

According to data of the present study the following conclusions are obtained:

- 1- The equilibrium isotherm for the system of adsorbed blue dye on activated carbon was of favorable type, and was well represented by Langmuir and Freundlich equations.
- 2- At flow rate (1.33 , 2 , 33.33 , and 60) $\times 10^{-3}$ m³/min the break through point time were (490 , 280 , 240 , and 130) min respectively, and the adsorption capacity were (39.32 , 37.29 , 34.86 , and 9.96) $\times 10^{-2}$ (kg/kg carbon) respectively.
- 3- At bed depth (10 , 20 , 30 , and 40) $\times 10^{-1}$ m the break through point time were (280 , 360 , 500 , and 630) min respectively, and the adsorption capacity were (37.29 , 44.02 , 54.33 , and 60.05) $\times 10^{-2}$ (kg/kg carbon) respectively.
- 4- At influent concentration (10 , 100 , 300 , and 500) ppm the break through point time were (400 , 400 , 360 , and 300) min respectively, and the adsorption capacity were (24.96 , 20.77 , 44.02 , and 74.82) $\times 10^{-2}$ (kg/kg carbon) respectively.
- 5- At particle size (0.6 , 1.18 , and 1.4) $\times 10^{-3}$ m the break through point time were (420 , 360 , and 330) min respectively, and the adsorption capacity were (70.02 , 59.99 , and 46.27) $\times 10^{-2}$ (kg/kg carbon) respectively.
- 6- The rate of mass transfer for initial stage of adsorption increased with increasing influent concentration and flow rate and also increased with decreasing particle size and bed depth.
- 7- The adsorption process using activated carbon insures an excellent degree of reduction for color with removal efficiency 90% .

- 8- The following correlations were obtained by applying multiple regression and represent the best fitting for the experimental data.

$$t = 0.41 - 0.3Q - 3.3C_0 + 8.8Z - 112.0 \text{ P.S}$$

$$q = 34.3 - 0.7Q + 1.3 C_0 + 0.9Z - 30.6 \text{ P.S}$$

- 9- The mathematical model that employed the resistance of external diffusion combined with surface diffusion fit well the experimental data.

5.2 Recommendations for further work:

The following recommendations can be helpful for further study:

- 1- This work can be extended to study the effect of pH and temperature on the capacity of activated carbon.
- 2- Testing another wastewater from other industries using the same treatment process, and a mixture solution of dyes.
- 3- The study can be extended using another type of adsorber like moving packed bed or fluidized bed adsorbers to show the performance of activated carbon.
- 4- Study the system pilot scale, and scaling up the designed data for adsorption units.
- 5- This study may be extended for using another type of adsorbents than activated carbon.

CHAPTER FOUR

RESULTS AND DISCUSSIONS

4.1 Langmuir and Freundlich Isotherm Equations:

Equilibrium isotherm had been determined and analyzed according to the Langmuir and Freundlich equations. The plot of (C_e/q_e) versus (C_e) shows a straight line in Fig (4-1).

This means that the equilibrium results are correlated well with the Langmuir's equation. The value of (\bar{Q}) and the Langmuir constant (b) were calculated from the slope and the intercept of the straight line Fig (4-1), these values were tabulated in table (4-1).

Fig (4-1): parameters for the Langmuir's equation

The plot of $(\log q_e)$ versus $(\log C_e)$ for the same equilibrium results showed a straight line in Fig (4-2); this means that the equilibrium data for the adsorption are correlated well with Freundlich's equation.

The Freundlich's equation constant (k) and $(1/n)$ were calculated from the slope and intercept of the straight line in Fig (4-2); these values were tabulated in table (4-1).

Fig (4-2): parameters for the Freundlich's equation

Figure (4-3) shows a comparison between the experimental and theoretical results, using Langmuir or Freundlich adsorption isotherm equations and shows favorable type of adsorption for experimental results.

Fig (4-3): Experimental and theoretical data were obtained from the Langmuir's and Freundlich's equations for the adsorption ratio

Table (4-1) Langmuir and Freundlich equation constants.

Equations	\bar{Q} (kg/kg)	b (m ^r /kg)	K (kg/kg)	1/n (m ^r /kg)	St. Err.	Corr. Coeff. (R)

Langmuir	0.010	96			4.47	0.99
Freundlich			7.08	0.74	7.84	0.97

4.2 Column Experiments:

Sixteen column experiments were carried out to study the effect of various initial conditions on the performance of the activated carbon column of adsorption reactive blue dye from aqueous solution. The relevant details of the experiments were tabulated in table (3-3).

The sample of calculation was shown in Appendix (B) and the results were listed in Appendix (E).

4.2.1 Effect of Flow Rate:

Four experiments, [Nos. (1-4), table (3-3)] were carried out at different flow rates (1.33, 2, 33.33, 60) m^3/min respectively and at a given initial dye concentration ($C_0=30$) ppm, bed depth (1.0) m, and particle sizes (0.6-1.4) mm

The break through curves for the above experiments results were plotted Fig (4-4), (effluent dye concentration versus time for a given flow rate). It can be seen from Fig (4-4) that as the flow rate of wastewater increased, the break through point time of the curve decreased, and from these results the flow rate of wastewater was found to be less than (20) m^3/min at a given other conditions.

To show the effect of wastewater flow rate on the adsorption ratio, Fig (4-5) represents adsorption ratio (weight of adsorbed /weight of carbon) versus time.

Fig (4-4): Break through curves of isotherm adsorption for different wastewater flow rate ($C_0=30$ ppm, $Z=1.0$ m, P.s=(0.6-1.4) mm)

Fig (4-5): Adsorption ratio curves for different wastewater flow rate
($C_0=30$ ppm, $Z=1.5 \times 10^{-2}$ m, $P.S=(0.6-1.4) \times 10^{-2}$ m)

Examining Fig (4-5), it can be seen that the adsorption ratio of higher wastewater flow rate is much faster than that for the lower one; this is due to phenomena at high wastewater's flow rate which causes a good disturbance for laminar sub-layer just over the carbon particle.

Also it can be observed that the lower the flow rate the longer the linear portion of the curve, indicating that film diffusion remains rate limiting for longer periods, while increasing flow rate in this region causes reduction to the surface film, thereby decreasing resistance to mass transfer so deviation from linearity occurs because of the increasing influence of intraparticle transport on the overall rate of mass transfer when the external surface area becomes essentially saturated with solution.

For constant bed diameter and bed depth, the increasing of wastewater's flow rate will effect the value of linear velocity and contact time, i.e. the increasing flow rate leads to the increasing linear velocity but the decreasing the contact time, where is necessary to reach velocity value less than (0.3) m/min. (44)

The effect of flow rate on the adsorption capacity of activated carbon was shown in Fig (4-6), by plotting the adsorption capacity [maximum values of each curve in Fig (4-5)] against wastewater's flow rate.

This Fig (4-6) shows that the adsorption capacity (accumulative adsorption rate) of activated carbon decreases as the flow rate of wastewater increases. This was due to a good available contact time which will affect the amount of the capacity, that for low flow rate the wastewater molecules would have a sufficient contact time to occupy the space within the particles.

The rates of mass transfer were obtained from the slopes of the linear portions of the adsorption ratio curves Fig (4-5). The relation between mass transfer rate and flow rate was represented in Fig (4-7).

This Fig (4-7) shows that the mass transfer rate increases as the flow rate of wastewater increases. Increased flow rate in this region may be expected to give a compression or reduction of the film thickness. Thereby decreasing resistance to mass transfer and increasing the mass transfer rate. Experimental results were tabulated in table (E-5), Appendix E.

Fig (4-6): Effect of the Wastewater's flow Rate on the Adsorption Capacity of Activated Carbon ($C_0=30$ ppm, $Z=1.0 \times 10^{-2}$ m, $P.s=(0.6-1.4) \times 10^{-3}$ m)

Fig (4-7): Effect of the wastewater's flow rate on the rate of mass transfer ($C_0=30$ ppm, $Z=1.0 \times 10^{-2}$ m, $P.s=(0.6-1.4) \times 10^{-3}$ m)

4.2.2 Effect of the Influent Concentration:

Four experiments [Nos. (4-8), table (3-3)] were carried out at different influent dye concentrations, (10, 100, 300, and 500) ppm respectively, while other parameters are constant, wastewater flow rate ($= 2.0 \times 10^{-2}$ m³/min), bed depth ($= 2.0 \times 10^{-2}$ m) and particle size ($= 0.6 - 1.4) \times 10^{-3}$ m.

The breaks through curves for the above experiments were plotted in Fig (4-8) by plotting the effluent dye concentration versus time. Fig (4-8) showed that the break through point was reached fast when the influent dye concentration increased, this means that the curves rise sharply for the concentration above (50 ppm) because the required time to reach the break through point is inversely related to the influent concentration of dye.

To show the adsorption ratio at different influent concentrations of dye, the solute adsorbed (the uptake) versus time were plotted in Fig (4-9). This figure shows that the total quantity of solute removed from solution at any period of time increased with increasing influent dye concentration. A linear portion exists for each curve at the early period of the experiments, this means that only external mass transfer resistance (film diffusion) is rate determining step because there is no concentration gradients within the particle, with increasing influent concentration the linear segment of the curves extends over a shorter period of time.

This observation coincides with the consideration that film diffusion controls as the rate limiting step to a point at which the external surface area becomes essentially saturated. Deviation from linearity occurs because of the increasing influence of intraparticle transport on the overall rate of mass transfer as each run progresses. (30)

The effect of influent concentration on the adsorption capacity of activated carbon was shown in Fig (4-10), by plotting the adsorption capacity [maximum values of each curve in Fig (4-9)] versus the different concentration.

Figure (4-10) showed that the adsorption capacity of activated carbon increased as the influent concentration of dye increased which acts as driving force, i.e. increasing the concentration difference (the difference between the dye's concentration in the bulk of solution and corresponding dye's concentration on the surface of the carbon particles).

Fig (4-8): Break through curves of isotherm adsorption for different influent concentration of dye ($Q=2.5 \times 10^{-2}$ m³/min, $Z=2.5 \times 10^{-2}$ m, $P.s=(0.6-1.4) \times 10^{-2}$ m)

Fig (4-9): Adsorption ratio curves of different influent concentration of dye ($Q=2.5 \times 10^{-2}$ m³/min, $Z=2.5 \times 10^{-2}$ m, $P.s=(0.6-1.4) \times 10^{-2}$ m)

Fig (4-10): Effect of different influent concentration on the adsorption capacity of activated carbon ($Q=2.5 \times 10^{-2}$ m³/min, $Z=2.5 \times 10^{-2}$ m, $P.s=(0.6-1.4) \times 10^{-2}$ m)

The rates of mass transfer for the initial stages of adsorption were obtained from the slopes of the linear portions of the curves in Fig (4-9). The relation between mass transfer rate and concentration was represented in Fig (4-10). This figure shows that the mass transfer rate increased with increasing influent dye concentration. The experimental results were tabulated in table (E-3), Appendix E.

Fig (4-11): Effect of influent dye concentration on the rate of mass transfer ($Q=2.5 \times 10^{-3} \text{ m}^3/\text{min}$, $Z=2.5 \times 10^{-2} \text{ m}$, $P.s=(0.6-1.4) \times 10^{-3} \text{ m}$)

4.2.3 Effect of Bed Depth:

Four experiments [Nos. (4-12), table (3-3)] were carried out at different activated carbon bed depths (10, 20, 30, and 40) $\times 10^{-2} \text{ m}$ respectively, while other parameters are constant: dye concentration (30 ppm), wastewater flow rate ($2.5 \times 10^{-3} \text{ m}^3/\text{min}$) and particle size ($=0.6-1.4$) $\times 10^{-3} \text{ m}$.

The breaks through curves for the above experiments were plotted (effluent dye concentration versus time for a given bed depth) as shown in Fig (4-12).

The break through points can not be seen clearly in Fig (4-12) except for bed depth (0.4 m); the break point is the value of exhaustion point where the value of effluent dye concentration is equal to influent concentration. This is because the total bed depth was smaller than the length of mass transfer zone. This figure showed also the increase of bed depth, which leads to increasing break through time.

To show the adsorption ratio at different bed depth of activated carbon, the solutes adsorbed versus time were plotted Fig (4-13). It can be observed from this figure that the total quantity of solute removed from solution at any period of time increases with increasing the bed depth.

When increasing bed depth, the total surface area that is available for adsorption will increase; this means that the service life of the carbon bed

increased with increasing of the carbon bed depth at constant flow rate of wastewater and constant linear velocity but the contact time will increase as bed depth increases.

Fig (4-12): Break through curves of isotherm adsorption for different bed depth of activated carbon ($Q=2.1 \times 10^{-6}$ m³/min, $C_0=3$ ppm, $P.s=(0.6-1.4) \times 10^{-3}$ m)

Fig (4-13): Adsorption ratio curves for different bed depth ($Q=2.1 \times 10^{-6}$ m³/min, $C_0=3$ ppm, $P.s=(0.6-1.4) \times 10^{-3}$ m)

The effect of bed depth on the adsorption capacity of activated carbon was shown in Fig (4-13), by plotting the capacity versus different bed depth.

Figure (4-13) showed that increasing bed depth would increase the capacity because additional spaces will be available for the wastewater molecules to be adsorbed on these unoccupied areas. Furthermore, increasing bed depth will give a sufficient contact time for these molecules to be adsorbed on the activated carbon surface.

Fig (E-14): Effect of different bed depth on the adsorption capacity of activated carbon ($Q=2.5 \times 10^{-3} \text{ m}^3/\text{min}$, $C_0=3 \text{ ppm}$, $P.s=(0.6-1.4) \times 10^{-3} \text{ m}$)

Plotting the slopes of adsorption ratio curves of Fig (E-13) against bed depth is shown in Fig (E-14).

This curve shows that the decrease of mass transfer rate is correlative with increasing carbon bed; this indicates that deeper bed leads to the increase in the required time to reach the saturation of carbon bed. The experimental results were tabulated in table (E-4), Appendix E.

Fig (4-10): Effect of different bed depth of activated carbon on the rate of mass transfer ($Q=2.1 \times 10^{-3} \text{ m}^3/\text{min}$, $C_0=3 \text{ ppm}$, $P.s=(0.6-1.4) \times 10^{-2} \text{ m}$)

Experiment (No. 13) was carried out for wastewater that effluents from the treatment plant unit of the textile factory. The break through curve of the experiment result was plotted in Fig (4-16).

When comparing this figure with Fig (4-12), which has the same experimental conditions ($Q=2.1 \times 10^{-3} \text{ m}^3/\text{min}$, bed depth = $2.1 \times 10^{-2} \text{ m}$, $p.s. = 0.6-1.4 \times 10^{-2} \text{ m}$, conc.=3 ppm), we can show that the break through point ($0.1 C_{inf}$) was reached in the same time, but the time of exhaustion point ($0.9 C_{inf}$) longer in Fig (4-16), because the presence of other pollutants like (chloride, sulphate,), affected the adsorption process but not adsorbed.

Fig (4-16): Break through curves of isotherm adsorption for industrial wastewater ($Q=2.5 \times 10^{-3} \text{ m}^3/\text{min}$, $C_0=30 \text{ ppm}$, $Z=2.5 \times 10^{-2} \text{ m}$, $P.s=(0.6-1.4) \times 10^{-3} \text{ m}$)

4.2.4 Effect of Particle Size:

Thirteen experiments [Nos. (1-13), table (3-3)] were carried out at the same particle size of activated carbon [i.e. mixed particle of size $(0.6-1.4) \times 10^{-3} \text{ m}$].

Three experiments [Nos. (14-16), table (3-3)] were carried out at different particle size $(0.6, 1.1, 1.4) \times 10^{-3} \text{ m}$, while other parameters are kept constant, dye concentration (30 ppm), wastewater flow rate ($2.5 \times 10^{-3} \text{ m}^3/\text{min}$) and bed depth ($=2.5 \times 10^{-2} \text{ m}$).

The break through curves for the above experiments were plotted through Fig (4-17), by plotting the effluent dye concentration versus time. Figure (4-17) showed that the required time for reaching the break through point increased when particle size decreased, this due to the fact that when the particle size decreases the surface area will be available for adsorption increased for a given adsorbent weight (i.e. providing more space for the dye

molecules to occupy the new surface area therefore it will increase the time of saturation).

Fig (4-17): Break through curves of isotherm adsorption for different particle size activated carbon ($Q=2.5 \times 10^{-5} \text{ m}^3/\text{min}$, $C_0=30 \text{ ppm}$, $Z=2.5 \times 10^{-2} \text{ m}$)

To show the adsorption ratio at different particle size, the solute adsorption versus time were plotted in Fig (4-18).

From Fig (4-18) it can be seen clearly that the quantity of dye adsorption per weight of activated carbon increases with decreasing of particle size; during the initial period of adsorption process there is an appearance different in accumulation value of quantity adsorption, while at later stages there was difference in values of quantity adsorption.

The effect of the particle size on the capacity of carbon was shown in Fig (4-19), by plotting the capacity versus different particle size. Examining Fig (4-19), it can be seen that increasing the particle size will decrease the adsorption capacity of the activated carbon. This was attributed to the fact that for small particles of activated carbon the micropores are believed to be more readily accessible by the wastewater molecules and the transport is mainly due to film diffusion which is more effective than intraparticle diffusion.

Fig (4-18): Adsorption quantity curves at different particle size of the activated carbon ($Q=2.5 \times 10^{-5} \text{ m}^3/\text{min}$, $C_0=3 \text{ ppm}$, $Z=2.5 \times 10^{-3} \text{ m}$)

Fig (4-19): Effect of particle size on the adsorption capacity of the activated carbon ($Q=2.5 \times 10^{-5} \text{ m}^3/\text{min}$, $C_0=3 \text{ ppm}$, $Z=2.5 \times 10^{-3} \text{ m}$)

As the particle size increases, the transport due to intraparticle diffusion will be more dominant, since it's slow and not very effective process, therefore the adsorption capacity will decrease when particle size increases as same as the rate of mass transfer will increase when the particle size decreases Fig (4-20). By plotting the rate of mass transfer versus different particle size.

The experimental results were tabled in table (E-6), Appendix E.

Fig (4-20): Effect of particle size on the rate of mass transfer ($Q=2.1 \times 10^{-2}$ m³/min, $C_0=3$ ppm, $Z=2.1 \times 10^{-2}$ m)

4.3 Development of Multiple Linear Regression Model:

By applying multiple linear regression (using SPSS system) to the experimental data in table (3-2) between the major independent variables (Q , C_0 , Z , and P.S) and the dependent variables (t , q) separately, the following correlation were obtained:

	Corr. Coef.
$t = 0.40 - 0.3Q - 3.3 C_0 + 1.8 Z - 112.0 \text{ P.S}$	0.92
$q = 34.3 - 0.7Q + 1.3 C_0 + 0.9 Z - 30.6 \text{ P.S}$	0.90

Where:

t : is time in (min) within the range of (130-630).

q : is the amount of adsorbate per unit weight of adsorbent in (kg/kg of carbon) within the range of $(9.96-74.82) \times 10^{-4}$.

Q : is the flow rate in (m³/min) within the range of $(1.33-6) \times 10^{-2}$.

C_0 : is the influent concentration in (ppm) within the range of (1-50).

Z: is the bed depth of activated carbon in (m) within the range of $(1.0-1.5) \times 10^{-2}$.

P.s: is the size of particle of activated carbon in (m) within the range of $(0.6-1.5) \times 10^{-3}$.

Verification for these equations can be made by plotting the experimental data which will not be included in the regression model versus modeling data as shown in Fig (4-21) and Fig (4-22); these figures showed that the experimental data are correlated well with the modeling data.

On the other hand we can made a general equation used as an indicator to compare the results of effluent concentration at any time of any variation in the same parameters used in this research and that will be entered in another similar work.

$$C = 0.668 t^{0.566}$$

Corr. Coe.

0.938

Fig (4-21): Verification for regression equation

Fig (4-22): Verification of regression equation

4.4 Predicting the Isothermal Adsorption Breakthrough Curves:

Design of the fixed bed column for adsorption involves predicting the concentration of the solute in the effluent as a function of time. The shape and time of appearance of “Break through curve” have a significant influence on the operation of the column. ⁽³⁷⁾

The mathematical model for fixed bed adsorber was used to predict the breakthrough curves of both external and intraparticle diffusion (surface diffusion) as described by Liaw et.al. ⁽³⁶⁾

The details of this model were presented in Appendix D and Computer program for the solution was shown in Appendix F.

Figures (ξ-23) to (ξ-27) represent a comparison between the experimental and predicted data obtained from the mathematical model for bed depths (1.0, 3.0)*10⁻² m, concentration (10, 30) ppm and flow rate (33.33*10⁻³) m³/min.

Figures (ξ-23 and ξ-24) present a comparison between theoretical and experimental data for 1.0*10⁻² m and 3.0*10⁻² m bed depths. These figures showed that the difference between the two curves was wider for longer bed depth (3.0*10⁻²) m.

A comparison between the theoretical and the experimental data for concentration (10 and 30 ppm) was presented in Figs (ξ-20 and ξ-26) respectively. A good agreement was obtained for the two curves in Fig (ξ-26), while for Fig (ξ-20) a good agreement was obtained until (10 min). After that time the difference was wider. This is due to that the value of surface diffusivity was assumed to be the same for both experiments. The effect of the surface diffusivity becomes pronounced at the later stage of the curves where the intraparticle diffusion becomes rate limiting. (30)

Figure (ξ-27) shows a comparison between the theoretical and the experimental data for flow rate (33.33*10⁻³) m³/min. The difference between the two curves was wider in the first stage, while a good agreement was pronounced at the later stage of the curves, this is due to the higher value of flow rate and the intraparticle diffusion becomes rate limiting at the later stage.

Fig (ξ-23): Experimental and predicted breakthrough curves for isothermal adsorption at bed depth (1.0*10⁻²) m, (Q=3.0*10⁻³ m³/min, C₀=30 ppm, P.s=(0.6-1.4)*10⁻⁷ m)

Fig (ξ-24): Experimental and predicted breakthrough curves for isothermal adsorption at bed depth (3.0*10⁻²) m, (Q=3.0*10⁻³ m³/min, C₀=30 ppm, P.s=(0.6-1.4)*10⁻⁷ m)

Fig (4-25): Experimental and predicted breakthrough curves for isothermal adsorption at $C=10$ (ppm), ($Q=2.5 \times 10^{-5}$ m³/min, $Z=2.5 \times 10^{-2}$ m, $P.s=(0.6-1.4) \times 10^{-2}$ m)

Fig (4-26): Experimental and Predicted breakthrough curves for isothermal adsorption at $C=30$ (ppm), ($Q=2.5 \times 10^{-5}$ m³/min, $Z=2.5 \times 10^{-2}$ m, $P.s=(0.6-1.4) \times 10^{-2}$ m)

Fig (4-27): Experimental and predicted breakthrough curves for isothermal adsorption at $Q=33.33 \times 10^{-5}$ (m³/min), ($C_0=30$ ppm, $Z=2.5 \times 10^{-2}$ m, $P.s=(0.6-1.4) \times 10^{-2}$ m)

The verification for these curves were shown below:

Fig (4-28): Verification for curve of $Z=1 \times 10^{-2}$ (m)

Fig (4-29): Verification for curve of $Z=3 \times 10^{-2}$ (m)

Fig (4-30): Verification for curve of $C=10$ (ppm)

Fig (4-31): Verification for curve of $C=30$ (ppm)

Fig (4-32): Verification for curve of $Q=33.33*10^{-3}$ (m³/min)

CHAPTER ONE

INTRODUCTION

1.1 Introduction:

Wastewater from the textile finishing industry can have a strong impact on the aquatic environment, because it is discharged in high quantity and may contain many biorecalcitrant contaminants. ⁽¹⁾ Many dyes used in textile industry are particularly difficult to remove by conventional waste treatment methods since they are stable to light and oxidizing agents, and are resistant to aerobic digestion. The removal of dyes in an economic fashion remains an important problem although recently a number of successful systems have been evolved using adsorption techniques. ⁽²⁾

There are several methods to remove color, these include sedimentation, using coagulants or polyelectrolytes, biological treatment, ultrafiltration, ion exchange, adsorption, chlorination or ozonation. ⁽³⁾

Activated carbon is an effective adsorbent primarily due to its extensive porosity and very large available surface area for adsorption. ⁽⁴⁾ Adsorption on activated carbon is used to any significant extent for the removal of dissolved organic from wastes and polluted waters. Adsorption was first observed by Scheele in 1773 for gases and subsequently for solutions by Lowitz in 1780. ⁽⁵⁾

Liquid-solid adsorption on activated carbon is characterized by slow rates and long periods between actions. The liquid flowing through an adsorber may be in contact with the carbon for a few minutes, such as when removing taste from water, or for several hours, as in the case of decolorizing sugar solutions. The granular carbon bed life may extend from a few days, for sugar solutions, to several years for taste removal. ⁽⁶⁾

The textile industry generally discharges its untreated and / or partially treated colored dye effluent into the sewer systems because of unavailability of an economically and technically favorable process. The discharge of such colored dye effluents is aesthetically objectionable, colored effluent also interferes with the transmission of sun light, even for a concentration of (1-2

mg/l) and upsets the biological metabolism processes, which causes the direct destruction of aquatic communities present in ecosystems. ^(v)

Furthermore, the color largely is unaffected by subsequent biological treatment methods. ^(^) Hence, stringent environmental protection laws have made the decolorization of dye effluent of prime importance before its discharge to ecosystems. The mounting pressure on the textile and dyeing industries for decolorization of their effluents has led to a search for a simple and cost – effective treatment process.

Reactive dyes are extensively used in textile and dyeing industries, but about 20-30% of input dyes remain in the mill wastewater. Because reactive dyes are highly soluble in water and difficult to remove from wastewater. ^(^) It was selected for this work some synthetic aqueous dye concentration solutions, which were used as model dye effluents.

Presently the textile – finishing industry in Hilla uses large quantities of water (1000 m³/day) and produces large volumes of aqueous effluent (800-1000 m³/day). Textile wastes are generally, colored, highly alkaline, high in BOD and suspended solids.

In the Hilla textile factor the wastewater treatment consists of screening, equalization, flocculation and neutralization, flotation, aeration then sedimentation. This treated solution requires further dye removal for disposal to river.

1.2 Aim of the Study:

Aim of this study is adsorption of blue dye on granular activated carbon from aqueous solution at constant temperature and pH by using continuous system (fixed-bed adsorber).

The effect of bed depth of activated carbon, particle size of granular carbon, wastewater flow rates and influent dye concentration was investigated in the research for fixed-bed adsorber.

Experimental and theoretical isotherm curves were determined and evaluating adsorption constants for Langmuir and Freundlich equations.

Batch process was used to estimate surface diffusivity experimentally and using ready mathematical equations to calculate the theoretical uptake fraction.

The study was developed a multiple linear regression model between the independent variables (Q, C_o, Z, P.S) and the dependent variables (t, q) separately. The above statistical correlations were done by using (SPSS V. 19.0 soft ware 1997) system.

The mathematical model used to predict the breakthrough curves was the external diffusion combined with surface diffusion resistance for different parameters.

CHAPTER TWO

LITERATURE REVIEW

AND THEORETICAL CONCEPT

2.1 Historical Review:

Activated carbon was first known to treat water over (2000) years ago. Adsorption by activated carbon has a long history of use in treating municipal, industrial and hazardous waste streams. Charcoal was used for drinking water filtration by ancient Hindus in India, and carbonized wood was used as a medical adsorbent and purifying agent by Egyptians. ⁽¹¹⁾

Powdered activated carbon was first produced commercially in Europe in the early 19th century, using wood as a raw material. This carbon found widespread use in the sugar industry. In the United States, the first production of activated carbon used black ash as the source, after it was accidentally discovered that the ash was very effective in decolorizing liquids. ⁽¹¹⁾

Activated carbon has since been used extensively for this purpose in many industries. In particular, it has been commonly used for the removal of organic dyes from textile wastewater.

In addition to its drinking water and wastewater treatment applications, activated carbon is used today for many other purposes some other common uses are listed here:- corn and cane sugar refining, gas adsorption, dry cleaning recovery processes, pharmaceuticals, fat and oil removal and electroplating.

Granular carbon filters were introduced in the (1930s) for the ultrapure of water in the food industry. ⁽¹²⁾

2.2 Textile Wastes:

Textile mill operations consist of weaving, dyeing, printing, and finishing. Many processes involve several steps, each contributing a particular type of waste, e.g. sizing of fibers, queering (alkaline cooking at elevated temperature), desizing the woven cloth, bleaching, mercerizing, dyeing, and printing.

Textile wastes are generally, colored, highly alkaline, high in BOD and suspended solids, and high in temperature. Wastes from synthetic- fiber manufacture resemble chemical. Manufacturing wastes and their treatment depend on the chemical process employed in the fiber manufacture. Equalization and holding are generally preliminary steps to the treatment of those wastes because of their variable composition, additional methods are chemical precipitation, trickling filtration, biological treatment and aeration.

The textile industry has long been one of the largest of water uses and polluters and there has been little success in developing low- cost treatment methods which the industry urgently needs to lessen the pollution loads it discharges to streams. ⁽¹³⁾

2.3 Adsorption:

Adsorption by solid is defined as the phenomena that take up of molecules from the fluid phase by the solid surface, the term (surface) includes both the (outer) geometric surface and (inner) surface bounding the capillaries, cracks and crevices. ⁽¹⁴⁾

The process can occur at an interface between any two phases such as, Liquid-liquid, gas-liquid, gas-solid, or liquid-solid interface. The material being concentrated or adsorbed is the adsorbate, and the adsorbing phase is termed the adsorbent. ⁽¹⁴⁾ The driving force of mass transfer solute from solvent to on the surface of solid adsorption may be the lyophobic (i.e. solvent- rejecting) character of the solute or the affinity of the solute for the solid or combination of both. ^(14,15)

If the bond that is formed between the adsorbate and adsorbent is very strong, the process is almost always irreversible, and chemical adsorption or chemisorption is said to have occurred. On the other hand if the bonds that are formed are very weak as is characteristic of bonds formed by Vander Waals forces, physical adsorption is said to have occurred. The molecules adsorbed by this means are easily removed or adsorbed, by a change in the solution concentration of the adsorbate and for this reason, the process is said to be reversible. Physical adsorption is the process that occurs most frequently in the removal of wastewater constituents by activated carbon. ⁽¹⁶⁾

Exchange adsorption is one of the types of adsorption that is used to describe adsorption characterized by electrical attraction between the adsorbent and the adsorbate that means (ion exchange). ^(17,18)

The heat of physical adsorption is usually in the range of (2-10) kcal/mol, and the heat of adsorption for chemisorption is usually in the range of (30-100) kcal/mol. ⁽¹⁹⁾

Abu Regebaa ⁽²⁰⁾, Studied the behavior of the fixed bed and fluidized bed isothermal adsorbers for the removal of the organic pollutant O- cresol from water by activated carbon, for the concentration of (100, 200, 300, 400, 500, 600, 700, 800, 900, 1000 mg/m³). Twenty-eight experiments were carried out to study the effect of various initial conditions (concentration, flow rate, bed depth, temperature, different linear velocities with constant contact time and type of beds on the performance of activated carbon. The equilibrium data were determined experimentally, and the equilibrium isotherm was found to be of a favorable type, and fit well Langmuir and Freundlich isotherms.

Shakir ⁽²¹⁾, used two different dye removal methods: chemical coagulation and adsorption through activated carbon. Adsorption through granular activated carbon was found to be very effective for the removal of the different dyes considered, where the percent dye removal was 96.7%, 98.7% and 98.5% for direct blue, sulphur black and vat yellow respectively. Equilibrium isotherm was found to be favorable type, and fit well Langmuir model for different dyes in water separately or in the dyes solution mixture.

Abood ⁽²²⁾, Studied the furfural removal from wastewater by the adsorption process by activated carbon using continuous system (fixed-bed). Nineteen experiments were carried out to study the effect of various initial conditions (bed depth, flow rate, particle size of activated carbon, and influent concentration) on the performance of fixed bed. The equilibrium data were determined experimentally and the equilibrium isotherm was found to be of a favorable type, and fit well Langmuir and Freundlich isotherms.

2.4 Adsorption Isotherm:

The adsorption isotherm is the equilibrium relationship between the adsorbate concentration in the fluid phase and the adsorbate concentration in the adsorbent particles at a given temperature.

A liquid phase isotherm shows the distribution of adsorbate between the adsorbed phase and the solution phase at equilibrium. It is a plot of the amount of adsorbate adsorbed per unit weight of carbon (q_e) versus the concentration of adsorbate remaining in the solution. ⁽¹⁹⁾ Fig (2-1)

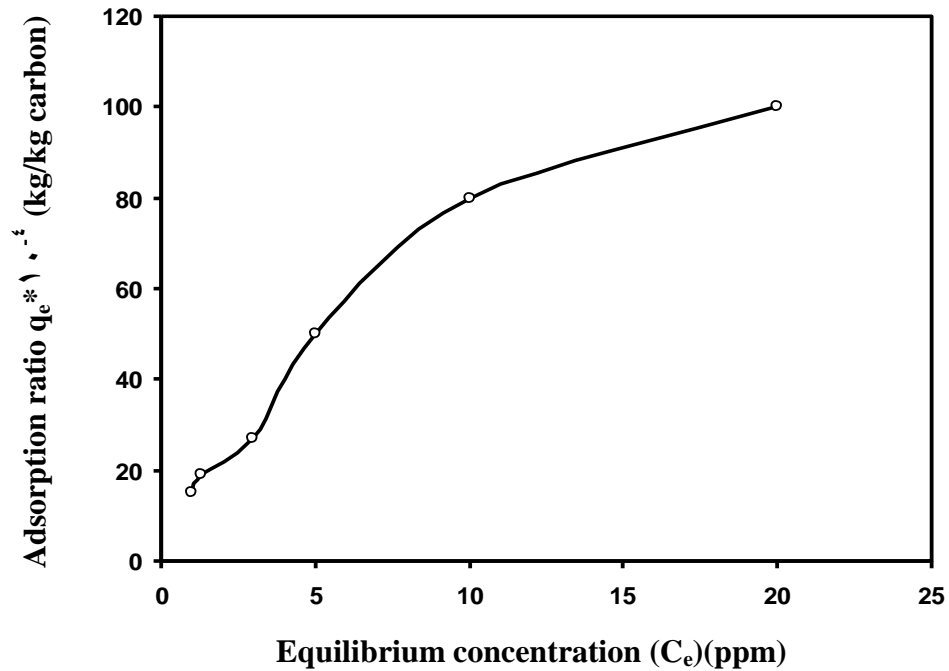


Fig (2-1): Adsorption isotherm for reactive blue dye on activated carbon

Commonly, the amount of adsorbed material per unit weight of adsorbent increases with increasing concentration, but not in direct proportion. Fig (2-2)

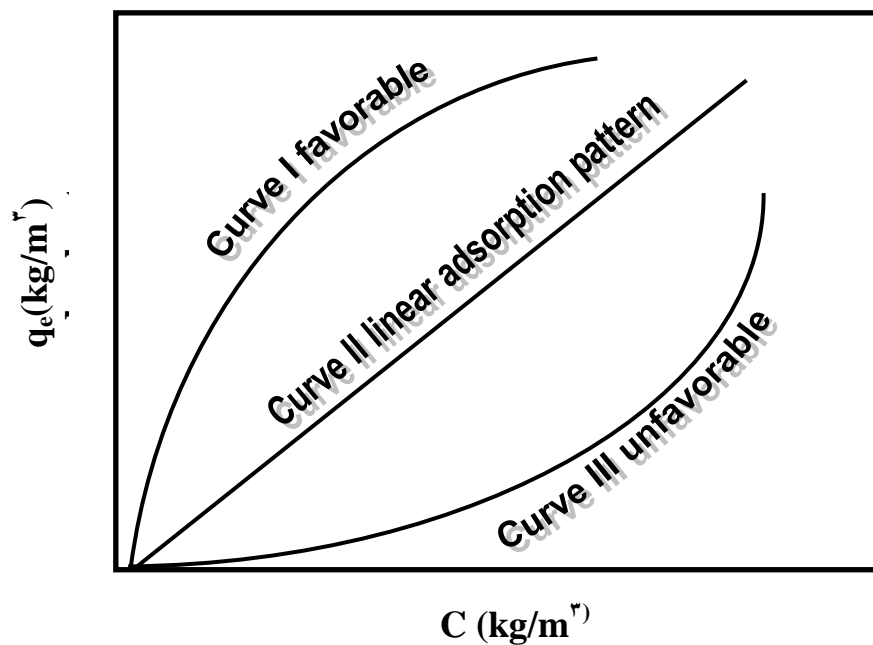


Fig (2-2): Types of sorption separations^(e)

Curves III and I indicate, for adsorption, curvilinear dependence of the amount concentrated at the solid surface on the amount remaining in the solution phase for favorable and unfavorable separation patterns respectively. Curve II represents a linear adsorption pattern. ⁽⁶⁾

2.0 Adsorption Equilibrium Relationships:

The mathematical formulation adsorption relationships are usually expressed in terms of either Freundlich or Langmuir equations.

The Freundlich equation has the general form: ^(10,11)

$$q_e = x/m = kC_e^{1/n} \quad \dots\dots(2-1)$$

Where:

q_e : Adsorption ratio at equilibrium. (kg/kg of carbon)

x : The mass of the adsorbate. (kg)

m : The mass of the adsorbent. (kg)

C_e : equilibrium concentration of the solute remaining in solution. (ppm)

K (kg/kg of carbon) and $1/n$ (m^3/kg): constants.

The equation which is more useful in logarithmic form is: ⁽¹²⁾

$$\log(q_e) = \log(x/m) = \log(k) + \frac{1}{n} \log C_e \quad \dots\dots(2-2)$$

A plot of (x/m) vs. concentration on Log-Log paper results in straight line with a slope of $(1/n)$ and an intercept (k). The intercept is roughly an indicator of sorption capacity and the slope of adsorption intensity.

Experimental data are often plotted in this manner as a convenient way of determining whether removal of material from solution is accomplished by adsorption and as means of evaluating the constant (k) and (n).

The Langmuir equilibrium adsorption equations has the form: ⁽⁶⁾

$$q_e = x/m = \frac{QbC_e}{(1 + bC_e)} \quad \dots\dots(2-3)$$

The linearization form of the equation is ⁽¹⁴⁾

$$C_e / q_e = 1/b\bar{Q} + C_e / \bar{Q}$$

.....($\gamma - \xi$)

Where:

\bar{Q} : The amount of adsorbate required to form a complete monolayer on the adsorbent surface. (kg/kg)

b: Constant related to the energy of adsorption. (m^r/kg)

A plot of (C_e / q_e) against (C_e) will give a straight line, the slope of which gives the value ($1/\bar{Q}$) and its intercept with the (C_e / q_e) axis is the value of ($1/\bar{Q}b$).

The Langmuir equation can be used for describing equilibrium for adsorption and for providing parameters (\bar{Q} and b) with which to quantitatively compare adsorption behavior in different adsorbate- adsorbent systems, or for varied conditions within any given system. ⁽⁵⁾

Kyte ^(7^A), obtained the constant (n) of Freundlich model which indicate to be favorable for isotherm when ($n > 1$). In these cases the solute is tending to a constant pattern and the adsorption fronts takes up a form whose shape does not change as it passes through the bed.

Poots, Mckay and Healy ^(7,7^o), found that the adsorption of dye (acid blue 7^o) on peat and wood conforms to both Freundlich and Langmuir equations. Langmuir parameters (\bar{Q} , b) and Freundlich parameters (k, n) for different particle sizes show increase in adsorption capacity with decrease in particle size.

Al-Bahrani and Martin ^(7^v), found that the equilibrium data for adsorption for many organic pollutants were correlated well with Langmuir and Freundlich equations, \bar{Q} was used to compare the carbon capacity for the adsorption of each solute. There appeared to be general tendency of increase in adsorption capacity with increase in molecular weight.

Martin and Al-Bahrani ^(7^v), found that the equilibrium data for adsorption for five organic pollutants were correlated well with the Langmuir equation. Comparison was made to show that the equilibrium capacity for each solute on the activated carbon was affected adversely by the presence of the other solutes.

2.1 Adsorption in Fixed Bed:

For fixed bed adsorption operation with activated carbon the water or wastewater to be treated is passed through a stationary bed of the carbon. An unsteady-state condition prevails in that the carbon continues to remove increasing amounts of impurities from solution over the entire period of useful operation. ^(*)

These adsorbers give the advantages simple operation plus the ability to serve as a filter for simultaneous suspended-solid removal. ^(*) The column can be operated either under pressure or by gravity. ^(**) Fig (2-3) is a plot of the adsorption pattern is normally obtained for a fixed-bed unsteady state adsorber. ^(*)

The solute or impurity is adsorbed most rapidly and effectively by the upper few layers of fresh carbon during the initial stages of operation. These upper layers are of course in contact with the solution at its highest concentration level, (C_0). The small amounts of solute which escape adsorption in the first few layers of adsorbent are then removed from solution in the lower strata of the bed, and essentially no solute escapes from the adsorber initially.

The primary adsorption zone is concentrated near the top or influent of the column. As the polluted feed water continues to flow into the column, the top layers of carbon become practically saturated with solute and less effective for further adsorption. Thus the primary adsorption zone moves downward through the column to regions of fresher adsorbent. The wave, like movement of this zone, accompanied by a movement of the (C_0) concentration front, occurs at a rate, which is generally much slower than the linear velocity of the water or wastewater.

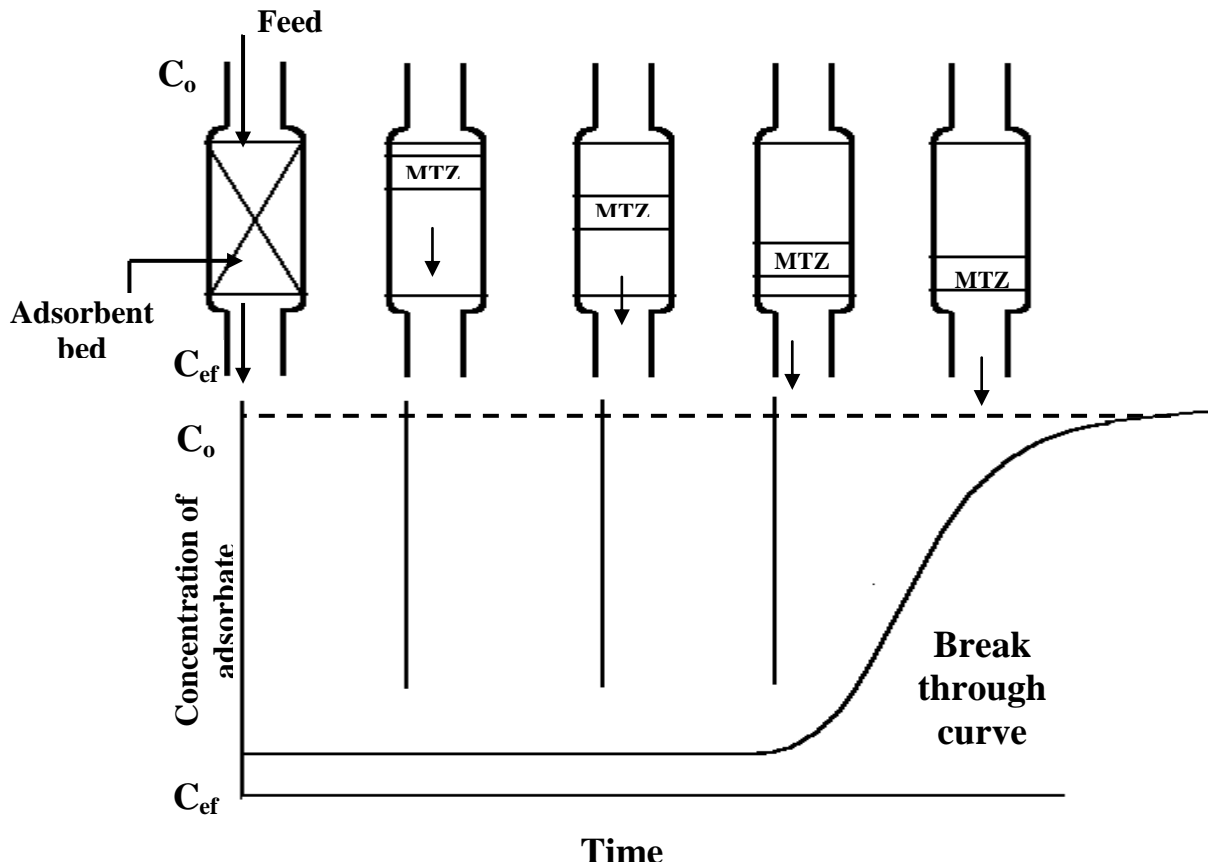


Fig (۲-۳): Schematic representation of the movement of the adsorption zone and the resulting breakthrough curve^(۲۲)

The plot of (C/C_0) versus time (for a constant flow rate) or volume of water treated depicts the increase in the ratio of effluent to influent concentrations as the zone moves through the column. The break point on this curve represents that point in operation where-for all practical purposes-the column is in equilibrium with the influent water, and beyond which little additional removal of solute will occur. At this point it is generally advisable to reactivate or replace the carbon.

Factors which affect the actual shape of the curve include the solute concentration, pH, and rate-limiting mechanism for adsorption, nature of the equilibrium conditions, particle size, the depth of the column of carbon and the velocity of flow.

As a general rule, the time to break through point is decreased by.^(۳۰)

- Increased particle size of the carbon.
- Increased concentration of solute in the influent.
- Increased pH of the water.
- Increased flow rate.

- Decreased bed depth.

If the total bed depth is smaller than the length of the primary adsorption zone required for effective removal of solute from solution, then the concentration of solute in the effluent will rise sharply from the time the effluent is first discharged from the adsorber.

The break through point is often taken as a relative concentration of (0.05 or 0.1) and since only the last portion of fluid processed has this high a concentration, the average fraction of solute removed from the start to the break point is often (0.99) or higher. (31)

2.7 Batch Processes:

Batch processes are important in which the adsorbent moves relatively to the walls of the containment vessel. The simplest process involves mixing a batch of adsorbent with a batch of fluid. (32)

Powdered or granular adsorbents are usually added to the equipment in slurry form in such a way as to allow adequate dispersion and mixing. When large quantity of adsorbent is required, consideration should be given for using a multiple batch or cross-flow system when the feed is first contacted with a fresh batch of adsorbent after separation of the fluid from the adsorbent, the fluid is contacted with a further fresh batch of adsorbent. (32)

2.8 Selection of Experimental Conditions:

2.8.1 Effect of Particle Size of Adsorbent:

For porous material such as activated carbon the breaking up of large particles to form smaller ones can in some instances serve to open some tiny, sealed channel in the carbon which might then become available for adsorption; this possibly yields the dependence of equilibrium capacity on particle size. (3)

In a liquid-phase application, transfer of the adsorbate from the bulk solution to the carbon particle must proceed through at least by two steps:

- 1- Film transport.
- 2- Intraparticle transport.

Kinetic experiments demonstrated that step 1 is appreciably more rapid than step 2. So the latter is normally the primary rate-determining step. The adsorption ratio then will vary with the diameter of the carbon particle used in the test. (10)

Weber (9), showed that the use of large particles of carbon, which may be removed more readily when exhausted in a system, required long periods of contact between solution and adsorbent, necessitating large basins or tanks in which to retain the water or waste during treatment.

Poots, Mckay and Healy (11,12), showed for a series of experiments that were carried out with different particle sizes, that in all cases the adsorption capacity increases with a decrease in particle size. This would appear to indicate that surface area associated with pores inside the particle is being at least partially occluded and that the effective adsorption regime is confined to the external surface and narrow layer just below the surface.

Martin and Al-Bahrani (13), observed a significant increase in adsorption capacity with decreasing carbon particle size and explained this due to the opening of new pores when crushing the carbon to small particles size.

Al-Tamemi (14), showed that the capacity of the activated carbon depends on the carbon particle size, possibly due to the fact that the pollutant molecules cannot completely penetrate all the pores within the carbon particles.

2.8.2 Effect of Influent Concentration:

The concentration of influent is one of the most important parameters that affect the adsorption process. It's consider a (driving force) of mass transfer process of molecule from fluid phase to the solid phase. It was noted that with increasing influent concentration, the linear segment of the solute uptake curve extended over a shorter period time. (10)

Both the mass transfer rate and the total quantity of solute removed from solution at any period of time increased with increasing influent concentration. (10)

Weber and Keinath (15), showed that with increasing influent concentration the linear segment of the solute uptake curve extended over a

shorter period of time; that is, film diffusion remains rate limiting for shorter periods of time.

Poots, Mckay and Healy ⁽¹⁹⁶⁰⁾, showed that the adsorption ratio uptake of acid dye decreases with decreasing the influent concentration and they showed that some adsorbent give the same result of effluent concentration for different influent concentration (10, 20, 30, 40 mg/l).

Martin and Al-Bahrani ⁽¹⁹⁷²⁾, showed that the rate uptake ($C_0 - C / C_0$) of γ -methyl pyridine decreases with decreasing of initial concentration, this is to be expected since the lower solute concentration will low the driving force for adsorption to occur.

2.8.3 Effect of Flow Rate:

For a number of different flow rates, the shape of break through curves at constant bed depth and other variables, which lead to variation with linear velocity. ⁽¹⁾

Weber and Keinath ⁽¹⁹⁶⁰⁾, illustrated that the effect of flow rate on the solute uptake is based on the assumption that film diffusion is rate limiting in early portions of a column run. Increased flow rate in this region may be expected to result in compression or reduction of the surface film, thereby decreasing resistance to mass transfer and increasing the mass transfer rate. The lower the flow rate the more marked is the influence of film diffusion and the longer the linear portion of the curve.

Poots and Mckay ⁽¹⁹⁶⁰⁾, found the treated volume of (50%), the break through curve time shows decreasing with increasing the flow rate at constant bed depth, diameter of bed and particle size.

McGuire and Suffet ⁽¹⁹⁷¹⁾, showed that when down flow velocity increases the capacity of activated carbon to adsorb organic reduces even though the contact time remained constant.

Crittenden and Thomas ⁽¹⁹⁷⁵⁾, indicated the empty bed contact time (EBCT) related with flow rate, when the flow rate increases the (EBCT) will decrease at constant volume of bed, where:

$$\text{Empty bed Contact time} = \frac{\text{Volume of Bed}}{\text{Flow Rate}} \dots\dots\dots(2-1)$$

2.8.4 Bed Depth:

Poots and Mckay ⁽²⁰⁾, found that difference in the shape of break through curves for varying the depth of bed at constant other variables.

Poots and Mckay ⁽²¹⁾, explained that the increase of breakthrough time of break curve occurs when the bed depth of the adsorbent increases.

Martin and Al-Bahrani ⁽²²⁾, showed that the service life of adsorbent column (carbon) increases with increasing bed depth and realized carbon adsorption capacity at break point increases at decreasing rate with increasing bed depth. This indicates that for deeper bed the contact time will increase.

2.9 Rate-Limiting Step:

The removal of dissolved substances from bulk liquid to the adsorption sites inside the adsorbent is usually described by one of the following transport mechanisms or by combination of them. ⁽²³⁾, Fig (2-4)

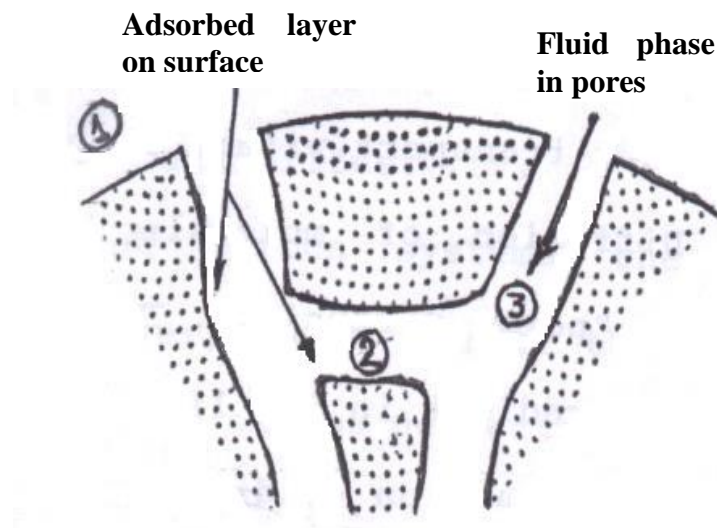


Fig (2-4): Modes of up take within adsorbent particle ⁽²³⁾

A-mass transfer from the bulk of the solution onto the outer surface of the particles, is called “film diffusion”.

Film diffusion is governed by molecular diffusion and, in turbulent flow, by eddy diffusion, which controls the effective thickness of the laminar boundary layer.

One logically may assume that the concentration of solute at a point in the boundary layer immediately adjacent to the external surface of the particle is in equilibrium with the average solid-phase concentration on the internal surfaces.

This condition may be stated algebraically as ⁽⁶⁾

$$\frac{dq}{dt} = k_m \alpha \left(\frac{e}{\rho_b} \right) (C - C_{eq}) \quad \dots\dots\dots(7-1)$$

Where:

q: Adsorption ratio at given time.	(kg/kg of carbon)
t: Time.	(min)
K _m : Mass transfer coefficient.	(m/s)
e: Void fraction of bed.	
ρ _b : Bulk density of bed.	(kg/m ³)
C: Dye concentration at given time.	(ppm)
α: Effective area for mass transfer across the fluid film per unit volume of bed.	(m ² /m ³)
C _{eq} : Concentration of dye at equilibrium	(kg/m ³)

If mass transfer is governed only by external resistance, there are no concentration gradients within the particle. ⁽⁷⁾

The applicability of the film-diffusion model is restricted to low concentration. ⁽⁸⁾

B- Mass transport within the particles:

I- Diffusion of molecules in the liquid filled pores is called “pore diffusion”. The driving force is the concentration gradient in the liquid in the pores.

The equation of diffusion for spherical particle may be written as ⁽⁹⁾

$$\frac{\partial q}{\partial t} + e_p \frac{\partial c}{\partial t} = D_p e_p \left(\frac{\partial^2 c}{\partial r^2} + \frac{2}{r} \frac{\partial c}{\partial r} \right) \quad \dots\dots\dots(\gamma-\nu)$$

Where:

e_p : Porosity of particle.

D_p : Pore diffusivity. (m²/s)

r : Radial distance from center of particle. (m)

It is assumed in this case that the diffusivity is independent of concentration.

II- Diffusion of molecules in the adsorbed state called solid or surface diffusion, is adsorption of the solute on the interior surfaces bounding the pore and capillary spaces. The adsorbed phase is assumed to consist of a layer of adsorbed molecules on the inner surface of the particle (the pore walls). The gradient of the solid phase concentration determines the transport. ^(٤٩)

The equation of diffusion for spherical particle in the case that the diffusivity is independent of concentration may be written as. ^(٤٠)

$$\frac{\partial q}{\partial t} + e_p \frac{\partial c}{\partial t} = D_s \left(\frac{\partial^2 q}{\partial r^2} + \frac{2}{r} \frac{\partial q}{\partial r} \right) \quad \dots\dots\dots(\gamma-\lambda)$$

Where:

D_s : Surface diffusivity. (m²/s)

For activated carbon systems the adsorbed phase concentration is very much larger than that in the pore walls and the latter can be neglected in the accumulation term. ^(٤١)

The surface diffusivity is strongly dependent on the concentration. ^(٤٢)
The relation for the more general case of a concentration dependent diffusivity is ^(٤٣)

$$\frac{\partial q}{\partial t} + e_p \frac{\partial c}{\partial t} = \frac{1}{r^2} \frac{\partial}{\partial r} r^2 D_s(q) \frac{\partial q}{\partial r} \quad \dots\dots\dots(\gamma-\rho)$$

Neretnicks ⁽⁴¹⁾, described the instationary transport in a sphere particle for simultaneous pore and surface diffusion with constant diffusion coefficient, by the following equation.

$$\frac{\partial q}{\partial t} = D_s \left(\frac{\partial^2 q}{\partial r^2} + \frac{2\partial q}{r\partial r} \right) + D_p e_p \left(\frac{\partial^2 c}{\partial r^2} + \frac{2}{r} \frac{\partial c}{\partial r} \right) \dots\dots\dots(41)$$

Fleck, Kirwan and Hall ⁽⁴²⁾, showed that the rate equation for the sorbent particle takes on different forms depending on the mechanism which controls the transfer of solute from the fluid phase into the solid phase-possible mechanisms which are: external plus pore diffusion, external plus solid diffusion, pore plus solid diffusion, and pore plus solid plus external diffusion.

The effective rate of adsorption evidently will be controlled chiefly by the step exerting greatest resistance to transfer, i.e. the slowest step. ⁽⁴³⁾

2.1. Kinetic of Adsorption:

When an adsorbent comes into contact with fluid, the number of molecules in the fluid decreases during their motion, the molecules strike the surface and some remain trapped on the surface for certain time then become adsorbed. ⁽⁴⁴⁾

The rate in which the numbers of molecules in fluid decrease depends on the velocity with which they reach site on the surface at which they are adsorbed.

For chemisorption the process of binding can be slow and complex, but for physical adsorption the mechanism of binding of the molecules has very high rate, and the factor controlling the rate of decrease of number of molecules in fluid phase (the overall rate of adsorption) is usually the rate of transport of the adsorbate to the sites on the surface at which they become bound. ⁽⁴⁵⁾

First the fluid molecules must reach the external surface of the adsorbent particle, there is no force, therefor, it is called (external diffusion). Under dynamic conditions when there is pressure drop in the system as a

result of motion of fluid, a connective flow (laminar or turbulent) must be considered.

When the molecules have reached the external surface of adsorbent particle, they can proceed to the internal surface by different ways, one of them is surface diffusion in narrow pores; the surface diffusion of adsorbed molecules becomes major importance. ⁽⁴⁴⁾

For investigation of adsorption kinetics, two different experimental methods have been used. ⁽⁴⁵⁾

- A-** Batch-type contact operation, in which a quantity of adsorbent is mixed continuously with a specific volume of wastewater until the pollutant in this solution has been decreased to desired level. The concentration profile decreases with the time as show in Fig (4-5).

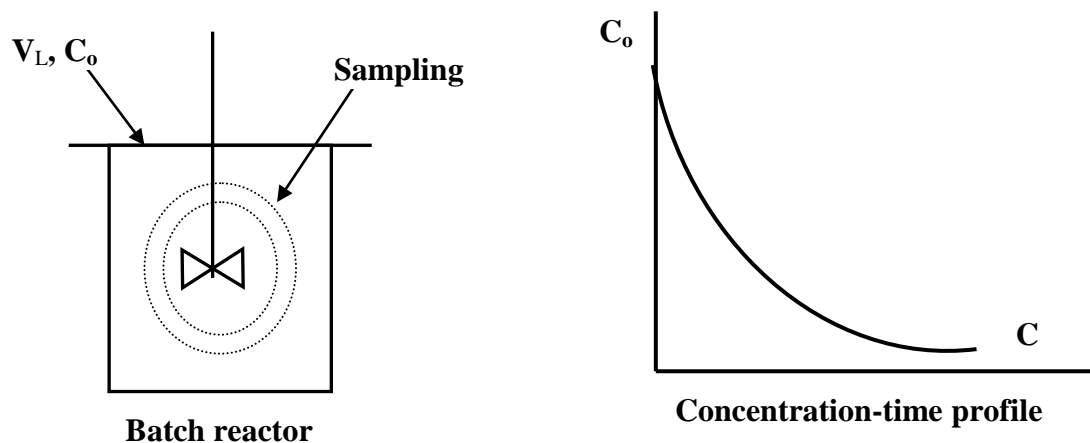


Fig (4-5): Schematic illustration of the experimental batch process ⁽⁴⁵⁾
 $(V_L$: Volume of solute (m^3), C_0 : Initial concentration of dye (ppm),
 C : Dye concentration at given time (ppm))

- B-** Column type (continuous-flow) operation in which aqueous solution with influent concentration flows from the top to the bottom or from the bottom to the top of the bed. The variation of the concentration in the water phase with the time at different bed length was measured.

Column type operation appeared to have distinct advantage over batch-type operations. For column operation the carbon is continuously in contact

with a fresh solution. Consequently, the concentration in the solution in contact with a given layer of carbon in a column is relatively constant. For

batch treatment, the concentration of solute, in contact with a specific quantity of carbon, steadily decreases as adsorption proceeds, thereby decreasing the effectiveness of the adsorbent for removing the solute. ⁽⁶⁾

2.1.1.1 Mathematical Model for Batch Adsorber:

In the case of aqueous systems, the adsorption quantity is controlled by diffusion of the solute into adsorbent particles.

Batch measurements were used to evaluate surface diffusivity and other parameters for performance of fixed bed.

Weber and Keinath ⁽⁴³⁾, showed that the film diffusion coefficient is measured of the resistance transfer of solute from bulk solution through the hydrodynamic boundary layer to the outer surface of adsorbent. No practical method determination of film diffusion coefficient in rapidly -agitated non-flow system is available.

Digiano and Weber ⁽⁶⁷⁾, developed a sorption model included the effects of mass transfer both at the external carbon-pollution interface and within the carbon pore structure.

$$N_{\sigma} = \frac{M_t}{R * C_{F0}} \quad \dots\dots(2-11)$$

Where:

M_t : Adsorbate uptake at given time (m mol/cm³).

R: Particle radius (cm).

N_{σ} : Total uptake at equilibrium (m mol/ cm³).

C_{F0} : Initial fluid phase concentration (mol/L).

Komiyama and Smith ^(45,46), developed a model based upon both pore-volume and surface transport and development a theory for correlating the surface diffusivity in term of heat of adsorption and free energy of activation for forming a vacant pore adjacent to an adsorbed molecules.

$$\frac{M_t}{M_{\infty}} = 1 - \sum_{n=1}^{\infty} \frac{6\theta(1+\theta)}{19\theta(1+\theta) + \theta^2 q_n^2} \exp[-q_n^2 TH] \quad \dots\dots(2-12)$$

Where:

$\frac{M_t}{M_\infty}$: Fractional uptake (amount of adsorbate at given time/ amount of adsorbent at equilibrium).

θ : Effective volume ratio.

q_n : Constants of theoretical model of batch process.

TH: Through put value dimensionless.

Suzuki and Kawazoe ⁽⁴⁴⁾, developed a simple technicality to determine the intraparticle diffusivities of adsorbents from concentration change in an agitated tank. Pore diffusion and a rectangular isotherm are assumed to derive the theoretical solutions.

Neretnicks ⁽⁴⁵⁾, solved numerically a mathematical model for finite bath adsorption of nonlinear isotherm which has been described by either the Langmuir or the Freundlich type equations. The transport mechanisms in the particles are assumed to be pore diffusion, solid diffusion or a combination thereof. The effect of film resistance is included.

Frits, Merk and schlunder ⁽⁴⁶⁾, showed that the resistance of external mass transfer is rate determining for low liquid concentration $< (0.1 \text{ m mol/l})$, and for higher liquid concentration the internal mass becomes increasingly important.

2.1.1.2 Measurement of Surface Diffusivity:

The surface diffusivity (D_s) was obtained by comparing experimental uptake data with theoretical uptake data. Experimental data were obtained using batch system as described by (Carman ⁽⁴⁷⁾, Grank ⁽⁴⁸⁾, Rice ⁽⁴⁹⁾, and Foo ⁽⁴⁴⁾). They illustrated that the diffusion into within the particle of adsorbent can be described by Fickian-type relationship:

$$\frac{\partial C}{\partial t} = D \Delta^2 C \quad \dots\dots\dots(2-13)$$

Where:

C: Concentration. (ppm)

t: Time. (min)

D: Diffusion coefficient. (m²/s)

The classical analytical solution for this relation depends on the shape of adsorbent particle, the final equation is as follows: ^{(1), (2)}

- For cylindrical particles.

$$\frac{W_o}{W_\infty} = 1 - \sum_{n=1}^{\infty} \frac{4\lambda(1+\lambda)}{4\lambda(1+\lambda) + \lambda^2 q_n^2} \exp[-q_n^2 TH] \dots\dots(2-18)$$

$$\lambda = (V_1 / k_e V_p) \text{ and } TH = (D_s t / R^2)$$

- For granular of uniform size and littler rounded shape can be approximated by sphere of radius (R).

$$\frac{W_o}{W_\infty} = 1 - \sum_{n=1}^{\infty} \frac{6\lambda(1+\lambda)}{9\lambda(1+\lambda) + \lambda^2 q_n^2} \exp[-q_n^2 TH] \dots\dots(2-19)$$

$$\lambda = (3 V_1 / 4\pi R^3)$$

q: Constants q₁, q₂

Where:

W_o / W_∞: Fractional up take (amount of adsorbate at given time/ amount of adsorbent at equilibrium).

λ: Effective volume ratio.

q_n: Constants of theoretical model of batch process.

TH: Through put value dimensionless.

V_p: Volume of adsorbent. (m³)

K_e: Sorption equilibrium constant.

R: Particle radius. (m)

By selecting mathematical model, theoretical (W_o/W_∞) will be obtained for each value of through put (TH>0) and value of time is being obtained from plot of experimental (W_o/W_∞) vs. time according to the theoretical values of (W_o/W_∞). Diffusion coefficient (D_s) will be obtained by relation of:

$$D_s = (TH R^2/t)$$

For each value of (TH) and time (t) when particle size (R) is known and average value of (D_s) will be estimated, as illustrated in Appendix C.

2.1.3 Mathematical Model for Fixed Bed Adsorber:

The same evaluation for model used in batch reactor tests applied for backed column experiments, only the different initial and boundary conditions for backed column operation must be considered. ⁽¹⁴⁾

Rosen ⁽¹⁵⁾, predicted a solution for the combined effects of intraparticle and external diffusion with linear equilibrium systems.

Weber and Keinath ⁽¹⁶⁾, made an initial approach toward characterization of rates of uptake of persistent organic pollutants from aqueous solution by active carbon in fluid-bed systems. An elementary but useful model for transfer has been utilized for quantifying the relative effects of selected systems variables- flow rate, particle size, solute concentration, pH and temperature- in terms of mass transfer rates and coefficients.

Liaw, Wang, Greenkorn and Choo ⁽¹⁷⁾, obtained a new solution to the kinetics of a fixed-bed adsorber in response to a step change in feed concentration for a linear equilibrium system with consideration for the resistance to mass transfer in both the mobile and stationary phases.

$$U_N = e^{\Theta+x} \left[1 + \sum_{i=1}^N \left[\prod_{k=1}^i \frac{\Theta}{k} \right] \left[1 + \sum_{j=1}^i \prod_{m=1}^j \frac{X}{m} \right] \right] \dots\dots\dots(2-17)$$

Where $\Theta = -\Theta/E$

$$x = -k_e X/E$$

x: Mass of adsorbate (kg).

K_e : Sorption equilibrium constant.

Θ : Relative time. (sec).

Johansson and Neretnicks ⁽¹⁸⁾, used three different techniques for determination of the kinetics. These were finite bath, infinite bath and fixed bed experiments.

Merk, Fritz and Schlunder ⁽¹⁹⁾, predicted a breakthrough behavior using alternatively three different models with different assumptions about

diffusion in the liquid filled pores and diffusion on the surface in series with external film diffusion.

According to the model of adsorption of adsorbate occurs at the outer surface, followed by diffusion within the carbon particle taking place in the adsorbed state:

$$n_{i,k} = \rho_k \delta_{i,k} \frac{\partial y_i}{\partial r} \dots\dots\dots(2-17)$$

Where:

ρ_k : Apparent particle density (g/cm³).

$\delta_{i,k}$: The diffusion coefficient, which describes the mobility of solute (i) in the particle, is obtained from batch reactor tests.

K: Mass of carbon (g).

n: flux (m mol/sec.cm²).

r: radial coordinate (mm).

Y: Concentration of adsorbate (m mol/g).

Rice⁽⁶⁷⁾, presented analytical solutions for three types of configurations batch, packed tube and radial-flow adsorbers. Experiments are used to test the theoretical predictions for batch and packed tube systems.

Abu Regabaa⁽⁷⁰⁾, used the mathematical model describing the transport of mass transfer from the bulk of the solution onto the outer surface of the particles (film diffusion), and found that there was no good agreement with the experimental data.

CHAPTER THREE

EXPERIMENTAL WORK

३.१: Material:

३.१.१ Adsorbate:

Reactive blue dye of chemical structure as shown in Fig. (३-१), with molecular weight (१३५g/mol) was used as adsorbate.

Dye wastewater enters the environment from dye manufacturers and dye consumers [e.g., textile, leather, and food industries], usually in the form of a dispersion or a true solution, and often in the presence of other organic compounds [chemical oxygen demand (COD)].^(३१)

The major environmental concern in treating wastewater from dying factories is the removal of color from the effluent. Untreated effluent from dying mills is usually highly colored and thus particularly objectionable if discharged into open water. Synthetic colorants represent a relatively large group of organic chemicals that are encountered in partially all spheres of our daily life. It is possible that such chemicals have undesirable effects, not only on the environment, but also on human health.^(३१)

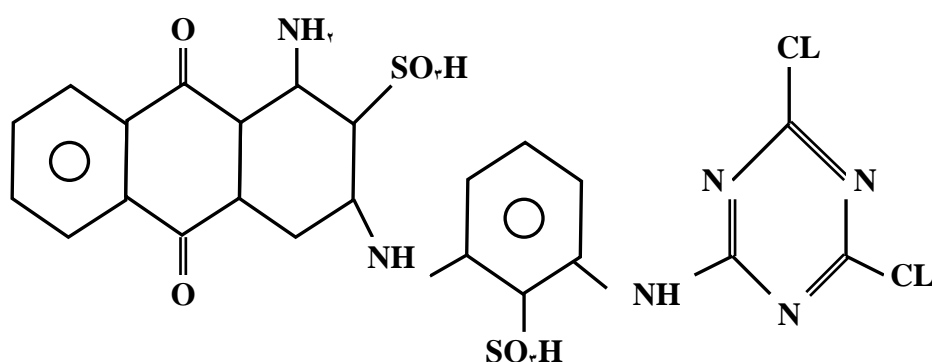


Fig (३-१): Molecular Structure of Reactive Blue Dye^(३१)

In order to minimize the possible damage to environment and human health arising from colored effluent, the dyeing industry is facing more stringent environmental regulations. The regulation of effluent standards for

color reduction is 10 (ppm) in Iraqi criteria. ^(v) Therefore, it is necessary for dyeing factories to install advanced treatment facilities to reduce effluent color and more stringent effluent standards. ^(vi)

Many dyeing factories currently use conventional wastewater treatment technologies such as activated sludge, chemical coagulation, and filtration. The drawback of these processes is that they are associated with the generation of large amounts of toxic sludge, which requires thermal combustion before final disposal and provides little or no efficiency in color degradation. ^(vii)

3.1.2 Adsorbent:

Granular activated carbon supplied by (unicarbo, Italian, Int. Co.) to Iraqi local markets was used as adsorbent with properties listed in table (3-1).

The unique structure of activated carbon produces a very large surface area (1 kg of activated carbon has surface area of 1000 m²). Activated carbon is manufactured by the carbonization and activation of carbonaceous material (animal or vegetable origin) which is almost exclusively of vegetable origin, such as wood, peat, coconut, coal, fruits stones and shells. ^(viii)

Activated carbon can be regenerated either chemically or thermally. In chemical regeneration, the carbon is contacted with chemicals that dissolve or oxidize the adsorbed impurities, while thermal regeneration proceeds by three major steps: vaporization of water near 100 °C, baking of the adsorbate at temperature up to 200 °C, and activation between temperatures of 200 and 300 °C. During the baking step, the organic adsorbates are converted to a volatile fraction and free carbon residues on the surface.

Activated carbon has specific properties depending on the material source and the mode of activation. ^(ix)

Activated carbon was sieved into various particle sizes within range of (0.6, 1.18, and 1.4) *10⁻³ m. The sieved carbon granular size was used in the present work to study the effect of various particle sizes on the adsorption process.

The carbon is firstly washed with distilled water and then dried in the oven at (110) °C for (3600 s). This time was usually enough to remove any undesired moisture within the particles.

Activated carbon has a large volume of very small pores, which creates a large surface area. These internal pores are classified based on size as either micropores (10^{-1000} A) or macropores (greater than 1000 A). Adsorption occurs primarily in the micropores with the macropores acting as conducts.

Table (3-1) Properties of Activated Carbon used in this Research

ITEM OF ANALYSIS	SPECIFICATION	RESULTS	METHOD
Dimensions (granular)	-	12*40 mesh(0.4-1.6)mm	
Bulk density(kg/m ³)	460-520	460-480	ASTM D 2804-96
Void fraction	-	0.40	
Surface area (m ² /gm)	1000(min)	1100-1130	ASTM D 4607-96
Hardness(%)	97(min)	98(min)	ASTM D 3802-94
Ash(%)	0(max)	0(max)	ASTM D 4607-94
Micropore	-	high	

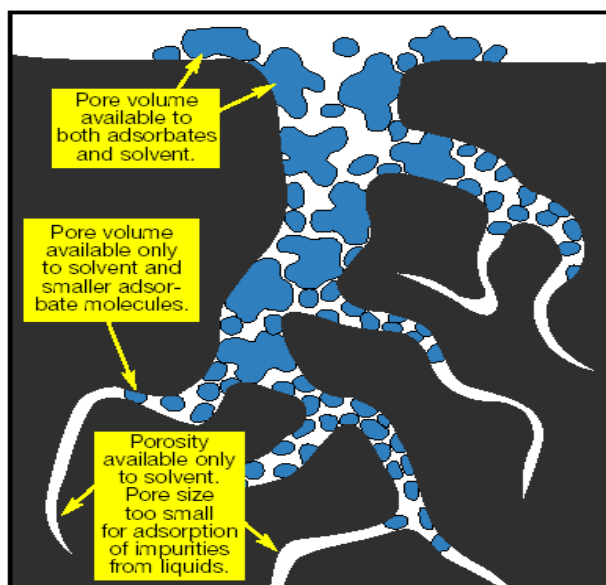


Fig (3-2): Exaggerated representation surface and pores of adsorbent⁽¹⁹⁾

3.1.3 Preparation of Samples:

The model dye solution was prepared by dissolving a weighed amount of the powder reactive blue dye (from textile factory) in tap water.

3.2 Experimental Arrangements:

3.2.1 Equilibrium Isotherm Experiment:

Granular activated carbon ranging in weight (0.1, 0.25, 0.5, 1.0, 1.5, and 2.0) g which are placed in individual six flasks of (100 ml) volume. The same volume of dye solution concentration (30 ppm) is added to each of the flasks and the flasks are placed in a shaker for about (8 h) at room temperature. The solution was filtered by filter papers, the filtrate was analyzed for dye concentration by spectrophotometer (CECIL CE 1000 SERIES).

The calibration curve for the concentration vs. absorbency of the dye used is given in Appendix A.

Plot of (q_e) amount of adsorbate per amount of carbon versus (C_e) concentration at equilibrium for each sample gives the experimental isotherm curve.

Plot of (C_e/q_e) vs. (C_e) to determine Langmuir constants (\bar{Q} , b), and plot of $(\log q_e)$ vs. $(\log C_e)$ to determine Freundlich constants (k, $1/n$), as described in section (2.1).

3.2.2 Column System (Continuous System):

Sixteen column experiments, table (3-2), were carried out at various initial conditions (flow rate, concentration, bed depth, and particle size). In all these experiments, the solution has pH=7, T=30°C, and followed the same procedure.

One experiment, table (3-3) experiment number (13), was carried out for raw water obtained from the effluent of treatment plant unit of the textile factory, and adjusted the desired dye concentration by additional powder reactive blue dye.

3.2.2.1 Equipment:

A schematic representation of experimental equipments are shown in Fig (3-3). A pilot unit is shown as photo in Fig (3-4).

A vertical Pyrex column was used as a fixed bed adsorber (0.1 m internal diameter), (1.1 m length). The activated carbon bed was confined in the column by means of the glass spheres placed on the top and bottom of bed to ensure a uniform distribution of influent wastewater through the carbon bed.

Two cylindrical tanks were used as container, the first one as a storage tank (1.1 m³), the second one as a feed tank (0.1 m³); each tank was fitted with gate valves.

An electronic four digital balance (sartorius R 200D) was used to weight the activated carbon and the solute (reactive blue). This weighted carbon is placed in the column to achieve the required bed height of (0.1, 0.2, 0.3, and 0.4) m respectively.

۳.۲.۲.۲ Procedure:

After preparing the solution with the desired concentration of solute (reactive blue dye) in the storage tank. This solution was pumped by means of centrifugal pump (type (KF-۲), SAER, ITALA) with capacity ۰.۰۰ (m^3/h) from the storage tank to the feed tank and then to the top of the column by gravity flow.

The adjustment of the flow rate to the desired value was obtained by volumetric method. Every (۱۰) minutes (۲ ml) sample was taken from the outlet of the column until equilibrium state was reached.

All experiments were carried out by changing one variable and keeping the others constant for a given run.

The break through data for reactive blue dye solution in water are tabulated in Appendix (E).

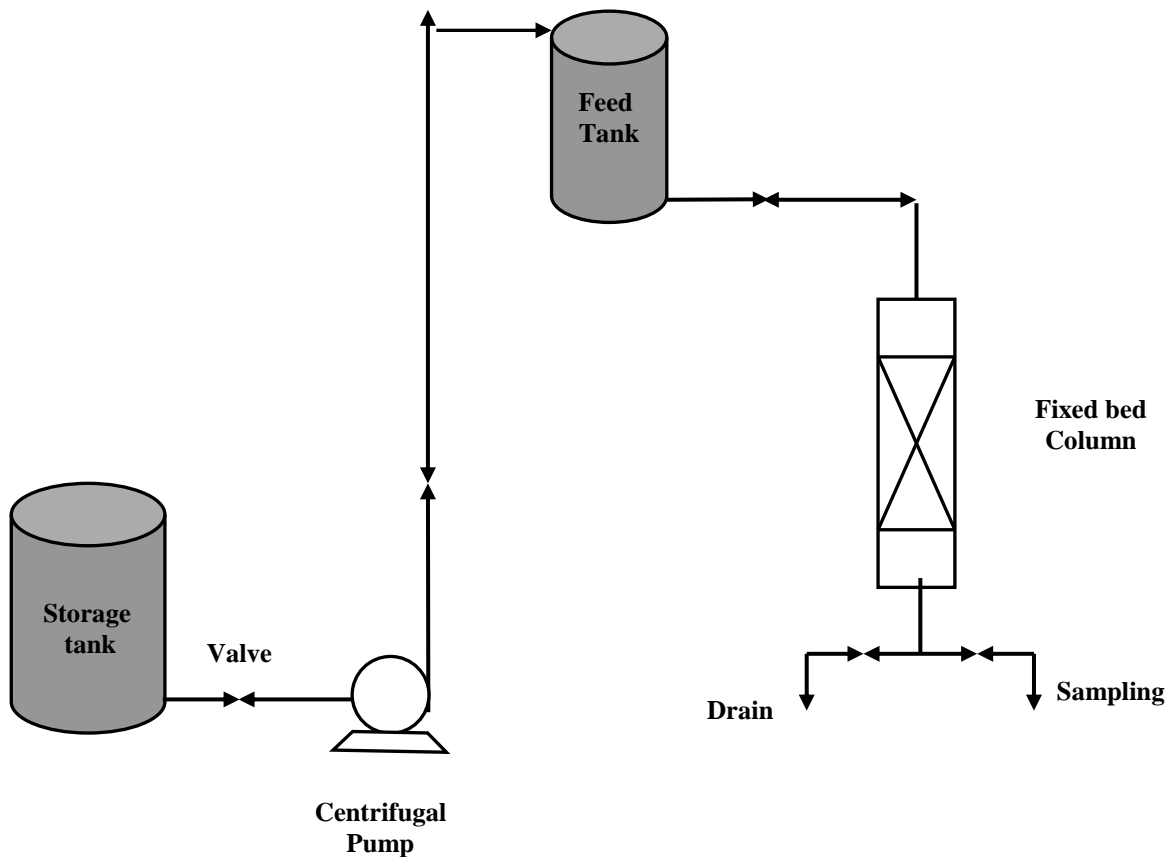


Fig (۳-۳): A schematic representation of experimental equipment

Table (۳-۲): Column system data

Exp. No.	Data of experimental					Data of results	
	$Q^* \text{ (m}^3/\text{min)}$	$C_0 \text{ (ppm)}$	$B.D^* \text{ (m)}$	$P.S. \text{ (m)}$	$M^* \text{ (kg)}$	$q^* \text{ (kg/kg)}$	Saturation time (min)
۱	۶.	۳.	۱.	۰.۶-۱.۴	۹۰	۹.۹۶	۱۳۰
۲	۳۳.۳۳	۳.	۱.	۰.۶-۱.۴	۹۰	۳۴.۸۶	۲۴۰
۳	۲.	۳.	۱.	۰.۶-۱.۴	۹۰	۳۷.۲۹	۲۸۰
۴	۸.۳۳	۳.	۱.	۰.۶-۱.۴	۹۰	۳۹.۳۲	۴۹۰
۵	۲.	۵.	۲.	۰.۶-۱.۴	۱۹۰	۷۴.۸۲	۳۰۰
۶	۲.	۳.	۲.	۰.۶-۱.۴	۱۹۰	۴۴.۵۲	۳۶۰
۷	۲.	۱۰	۲.	۰.۶-۱.۴	۱۹۰	۲۵.۷۷	۴۰۰
۸	۲.	۱.	۲.	۰.۶-۱.۴	۱۹۰	۲۴.۹۶	۴۶۰
۹	۲.	۳.	۴.	۰.۶-۱.۴	۳۸۰	۶۰.۰۵	۶۳۰
۱۰	۲.	۳.	۳.	۰.۶-۱.۴	۲۸۰	۵۴.۳۳	۵۵۰
۱۱	۲.	۳.	۲.	۰.۶-۱.۴	۱۹۰	۴۴.۵۲	۳۶۰
۱۲	۲.	۳.	۱.	۰.۶-۱.۴	۹۰	۳۷.۲۹	۲۸۰
۱۳	۲.	۳.	۲.	۰.۶-۱.۴	۱۹۰	۴۳.۲۶	۴۵۰
۱۴	۲.	۳.	۲.	۱.۴	۱۹۰	۴۶.۰۷	۳۳۰
۱۵	۲.	۳.	۲.	۱.۱۸	۱۹۰	۵۹.۹۹	۳۶۰
۱۶	۲.	۳.	۲.	۰.۶	۱۹۰	۷۰.۵۲	۴۲۰

۳.۲.۳ Batch System:

The batch system was utilized to estimate the average surface diffusivity (D_s). This was achieved by obtaining the initial concentration of the batch experiment identical to the influent concentration of the column experiment.

۳.۲.۳.۱ Equipment:

A Pyrex glass cylinder (1 liter) was used as a reactor container. The cylinder was fitted with a variable speed (1000 rpm) and magnetic stirrer (PROLABO).

3.2.3.2 Procedure:

An accurately weighed amount of activated carbon (0.1 kg) was placed into the cylinder. The cylinder contained (1 lit.) of an aqueous solution of (30 ppm) of reactive blue dye concentration. The activated carbon was immediately mixed with the solution by magnetic stirrer at room temperature and speed (1000 rpm). Every (10) minutes samples (3 ml) were taken out periodically by means of pipette for analysis until equilibrium is reached. The samples were filtered before the analysis using filter paper.

The concentration of the solute in the samples was determined by device of spectrophotometer. The results were plotted as (W_0/W_∞) (the quantity of adsorbate removed from bulk solution over the total quantity of adsorbate at equilibrium) versus time.

The surface diffusivity (D_s) was obtained by comparing the experimental and theoretical data.

Theoretical data are obtained by using the model described by equation (3.13). The detail for this procedure was presented in appendix C.

3.3 Analysis System:

3.3.1 Dye Concentration:

A (3 ml) sample was taken from the column and batch experiments every (10 min), for the analysis of the concentration of blue dye.

Samples were analyzed for absorbance using a variable wave length spectrophotometer type (CECIL CE 1000 SERIES) at the predetermined maximum absorbance wave length (λ_{max}) of the parent dye (determined using a scanning spectrophotometer) type (CINTRA GBC Scientific Equipment). The principle of spectrophotometry involves radiation being selectively absorbed when passed through a sample at a specific wavelength.

The degree of absorption, at the specific wavelengths, is directly proportional to concentration. Thus qualitative and quantitative determination

may be made by examination of spectrum and comparison of the absorption with that of known concentration standards.

3.3.2 Determination of other pollutants:

Sulphate was determined by titration with the solution of (Na₂EDTA) as well as amount of hydraulic acid and barium chloride. Dye (EBT) was used as an indicator. (14) While the chloride was measured by the method of titration with silver nitrate, by using botacium chromate as an indicator.

Total hardness was measured by titration with (Na₂EDTA) solution, by using merocresol dye (EBT) and ammonia solution at pH=10 as an indicator. Hardness is usually expressed in (ppm) of calcium carbonate, this is obtained by multiplying the total hardness by (0.5).

Calcium hardness was measured by the method of titration with (Na₂EDTA) solution, and using merocresol dye (EBT) and ammonia solution with pH=12 as an indicator.

Magnesium hardness was measured by
 $Mg = 0.5 \times \xi$ (total hardness – Calcium hardness). (15)

The results of this investigations were tabulated in Appendix E, table (E-6).

Fig (۳-۴): Photo of Experimental pilot plant

References:

- (1) Dieckhues, B., (1960): "Experiments on the reductive splitting of azo dyes by bacteria". J. ASCE, Vol.180, No.2. PP.244-249.
- (2) Poots, V. J. P., McKay, G. and Healy, J. J., (1976): "The removal of acid dye from effluent using natural adsorbents". J. Water Research, Vol.10, PP.1067.
- (3) McKay G. and McAleavey, G., (1988): "Ozonation and Carbon Adsorption in Three Fluidized Bed for Colour Removal from Peat Water". Chem. Eng. Res. Des., Vol.66, P.531.
- (4) Jason, P.P., (1999): "Activated Carbon and Some Applications for the Remediation of Soil and Ground Water Pollution". Naraine Persand, Virginia Tech.
- (5) Weber W. J., (1972): "physiochemical Processes for Water Quality Control". Wiley-Inter Science, New York.
- (6) Erskine, D. B. and Schuliger, W. G., (1971): "Activated carbon processes for liquid". Chem. Eng. Prog., Vol.67, No.11, PP.41.
- (7) Kuo, W.G., (1992): "Decolorizing Dye Wastewater with Fenton's Reagent". J. ASCE, Vol.26, No.7, PP.881-886.
- (8) Shu, H. and Huang, C., (1990): "Degradation of Commercial azo Dyes in Water using Ozonation an UV- enhanced Ozonation process". Chemosphere, J. ASCE, Vol.31, PP. 3813-3820.
- (9) William, A. R. and Leonard, T. F., (1997): "Water and Salt Reuse in the Dyehouse". Textile Chemist and Colorist, J. ASCE, Vol.29, No.4, PP.10-19.
- (10) Cheremisinoff, Paul, N. and Angelo, C., (1980): "Carbon Adsorption Applications". **Carbon Adsorption Handbook**. Ann Arbor Science Publishers, Inc. Ann Arbor, Michigan, PP. 1-5, www.Cee.Vt.edu.
- (11) Mantell, Chartes, L., (1968): "Activated carbon: surface chemistry and adsorption from solution". John Wiley and Sons, Inc. New York, www.Cee.Vt.edu.
- (12) David, W. J., (1986): "Dual Rate Kinetics". Env. Eng., Vol.17, P.440.
- (13) Atkins, M. H. and Lowe, J. F., (1979): "Case Studies in Pollution Control Measures in the Textile Dying and Finishing Industries". Pergamon Press, Oxford, New York.
- (14) Kirk R. E. and Othmer D. F., (1987): "Encyclopedia of Chemical Technology". Mack printing Co., Easton, U.S.A., Vol.1, PP.206-232.

- (١٥) Casey T. J., (١٩٩٢): **"Unit Treatment Processes in Water and Wastewater Engineering"**. Wiley Series, New York, "The International Conference on Water and the Environment".
- (١٦) Mitcalf and Eddy., (١٩٧٢): **"Wastewater Engineering : Collection, Treatment, and Disposal"**. McGraw-Hill, Book Company.
- (١٧) Rao C. S., (١٩٩٤): **"Environmental Pollution Control Engineering"**. Wiley Easton, ٢nd, India.
- (١٨) Ludersen A. L., (١٩٨٣): **"Mass Transfer in Engineering Practice"**. John Wiley and Sons, New York, ch. ٧.
- (١٩) Graham D., (١٩٥٩): **"Activated carbon regeneration"**. Chem. Eng. Prog. Symposium Series, Vol.٥٥, No.٢٤, PP. ١٧.
- (٢٠) Abu Regebaa, Y. A. Z. M., (١٩٩٢): **"Removal of pollutants from water by adsorption"**. M.Sc. Thesis, College of Engineering, University of Baghdad, Iraq.
- (٢١) Shakir, E. K., (٢٠٠٢): **"study of industrial wastewater treatment and recycling process for cotton-textile industry"**. D.ph. Thesis, College of Engineering, University of Baghdad, Iraq.
- (٢٢) Abood, W. M., (٢٠٠٤): **"Designing of pilot plant for treatment of wastewater contaminated by the furfural"**. M.Sc. Thesis, College of Engineering, University of Baghdad, Iraq.
- (٢٣) Martine, R. J. and Al-Bahrani, K. S., (١٩٧٩): **"Adsorption studies using gas-liquid chromatography-IV. Adsorption from bisolute-systems"**. J. Water Research, Vol.١٢, PP.١٢٠١-١٢٠٤.
- (٢٤) Abdul-Hammed, H. M., (١٩٩٦): **"Reduction of organic content in wastewater by adsorption onto activated carbon"**. M.Sc. Thesis, College of Eng., Univ. of Baghdad, Iraq.
- (٢٥) Poots V. J. P., Mckay, G. and Healy J. J., (١٩٧٦): **"The removal of acid dye from effluent using natural adsorbents"**. J. Water Research, Vol.١٠, PP.١٠٦١.
- (٢٦) Al-Bahrani, K. S. and Martin, R. J., (١٩٧٦): **"Adsorption studies using gas-liquid chromatography-I. Effect of molecular structure"**. J. Water Research, Vol.١٠, PP.٧٣١-٧٣٦.
- (٢٧) Martine, R. J. and Al-Bahrani, K. S., (١٩٧٧): **"Adsorption studies using gas-liquid chromatography-II. Competitive adsorption"**. J. Water Research, Vol.١١, PP.٩٩١.
- (٢٨) Kyte, W. S., (١٩٧٣): **"Nonlinear adsorption in fixed bed: The Freundlich isotherm"**. Chem. Eng. Sci., Vol.٢٨, PP.١٨٥٣-١٨٥٦.
- (٢٩) Martin, R. L. and NG W. J., (١٩٨٥): **"Chemical regeneration of exhausted activated carbon-II"**. J. Water Research, Vol.١٩, No.١٢, PP.١٥٢٧-١٥٣٥.

- (३०) Treybal, R. E., (१९८१): “**Mass Transfer Operations**”. McGraw Hill, Inc., New York.
- (३१) McCabe, W. I., Smith, J. C. and Hariott, P., (१९९१): “**Unit Operation of Chemical Engineering**”. १th ed. McGraw Hill.
- (३२) Crittenden, B. and Thomas, W. J., (१९९८): “**Adsorption Technology and Design**”. Butter Worth and Heinemann, Woburn, UK.
- (३३) Martine, R. J. and Al-Bahrani, K. S., (१९९८): “**Adsorption studies using gas-liquid chromatography-III. Experimental of factors influencing adsorption**”. J. Water Research, Vol.१२, PP.८९९-९०८.
- (३४) Al-Tamemi, A. R., (१९८०): “**Parameters affecting adsorption of phenol form**”. J. Water Research, Vol.१९, PP.४९१.
- (३०) Weber, W. J., Jr. and Keinath, T. M., (१९६९): “**Mass transfer of perdurable pollutants from dilute aqueous solution in fluidized adsorbers**”. Chem. Eng. Prog. Symposium Series, Vol.६३, No. ९४, PP. ९९.
- (३६) Mcguire, M. J. and Suffet, I. H., (१९८०): “**Activated carbon adsorption of organic from the aqueous phase**”. Vol.२, PP.१३९, Ann Arbor, Science Publishers, Michigan.
- (३७) Fleck, R. D., Kirwan, D. J. and Hall, K. R., (१९९३): “**Diffusion process in adsorption system**”. Ind. Eng. Chem. Fundam., Vol.१२, PP.९०.
- (३८) Merk, W., Fritz, W. and Schlunder, E. U., (१९८१): “**Competitive adsorption of two dissolved organic onto activated carbon-II**”. Chem. Eng. Sci., Vol.३६, No.४, PP.९४३.
- (३९) Merk, W., Fritz, W. and Schlunder, E. U., (१९८१): “**Competitive adsorption of two dissolved organic onto activated carbon-II**”. Chem. Eng. Sci., Vol.३६, No.४, PP.९३१.
- (४०) Johansson, R. and Neretnicks, I., (१९८०): “**Adsorption on activated carbon in countercurrent flow an experimental study**”. Chem. Eng. Sci., Vol.३०, PP. ९९९.
- (४१) Neretnicks, I., (१९९६): “**Analysis of some adsorption experiments with activated carbon**”. Chem. Eng. Sci., Vol.३१, PP.१०२९.
- (४२) Neretnicks I., (१९९६): “**Adsorption in infinite bath and countercurrent flow with systems having a concentration dependent coefficient of diffusion**”. Chem. Eng. Sci., Vol.३१, PP.४६०.
- (४३) Weber, W. J. and Keinath, T. M., (१९६८): “**A predictive model for the design of fluid-bed adsorber**”. W. P. C. F. J., Vol.४०, No.०.
- (४४) Milan, S. and Slavoj, C., (१९९०): “**Activated carbon**”. Elsevier pub. Co., Amsterdam.

- (٤٥) Suffet, I. H. and Mcguire, M. J., (١٩٨٠): **“Activated carbon adsorption of organic from the aqueous phase”**. Vol.١, PP.١٩٣, Ann Arbor, Science publishers, Michigan.
- (٤٦) Neretincks, I., (١٩٧٦): **“Adsorption in infinite bath and countercurrent flow with systems having nonlinear isotherm”**. Chem. Eng. Sci., Vol.٣١, PP.١٠٧.
- (٤٧) Komiyama, H. and Smith, J. M., (١٩٧٤): **“Surface diffusion in liquid-filled pores”**. A. I. Ch. E. journal, Vol.٢٠, No.٦, PP.١١١٠-١١١٧.
- (٤٨) Komiyama, H. and Smith, J. M., (١٩٧٤): **“Intraparticle mass transfer in liquid-filled pores”**. A. I. Ch. E. journal, Vol.٢٠, No.٤, PP.٧٢٨-٧٣٤.
- (٤٩) Suzuki, M. and Kawazoe, K., (١٩٧٤): **“Chromatographic study of diffusion in molecular-sieving carbon”**. Chemical Engineering of Japan, Vol.٧, No.٥, PP. ٣٤٦.
- (٥٠) Digiano, F. A. and Weber, W. J., (١٩٧٣): **“Sorption kinetics in infinite-bath experiments”**. W. P. C. F. J., Vol.٤٥, No.٤, PP.٧١٣.
- (٥١) Carman, P. C. and Houl, R. A., (١٩٥٤): **“Measurement of diffusion coefficient”**. J. Proc. Roy. Soc., ٢٢٢A, PP.١٠٩.
- (٥٢) Grank, J., (١٩٥٧): **“The mathematical of diffusion”**. PP.٨٤, Amen House, London.
- (٥٣) Rice, R. G. and Foo, S. C., (١٩٧٩): **“Sorption equilibria and equilibrium studies”**. Ind. Eng. Chem. Fundam., Vol.١٨, No.١, PP.٦٣-٦٧.
- (٥٤) Foo, S. C. and Rice, R. G., (١٩٧٩): **“Sorption equilibria and rate studies”**. Ind. Eng. Chem. Fundam., Vol.١٨, No.١, PP.٦٨-٧٥.
- (٥٥) Rosen, J. B., (١٩٥٤): **“General numerical solution for solid diffusion in fixed beds”**. Ind. Eng. Chem., Vol.٤٦, No.٨, PP.١٥٩٠.
- (٥٦) Liaw, C. H., Wang, J. S. P., Greenkorn, R. A. and Chao, K. C., (١٩٧٩): **“Kinetics of fixed-bed adsorption: A new solution”**. A. I. Ch. E. J., Vol.٢٥, No.٢, PP. ٣٧٦.
- (٥٧) Rice, R. G., (١٩٨٢): **“Approximate solutions for batch, packed tube and radial flow adsorbers-comparison with experiment”**. Chem. Eng. Sci., Vol.٣٧, No.١, PP.٨٣.
- (٥٨) Chiou, M. S., Yen Ho, P., and Ya Li, H., (٢٠٠٣): **“ Adsorption behavior of dye AAVN and RB٤ in acid solutions on chemically cross-linked chitosan beads”**. J. Chin. Chem. Engrs., Vol.٣٤, No.٦, PP. ٦٢٥-٦٣٤.
- (٥٩) Cooper, P., (١٩٩٥): **“Color in dyehouse effluent”**. J. ASCE, Alden Press, London.
- (٦٠) Philippe, C. V., Roberto B. and Willy V., (١٩٩٨): **“Treatment and reuse of wastewater from the textile wet-processing industry: Review of emerging technologies”**. J. ASCE, Vol.٧٢, PP.٢٨٩-٣٠٢.

- (٦١) Marmagne, O. and Coste, C., (١٩٩٦): “**Color removal from textile plant effluents**”. J. ASCE, Am. Dyestuff Rep. Vol.٨٥, PP.١٥-٢١.
- (٦٢) Ecknfelder, W. W., Jr., (١٩٦٦): “**Industrial water pollution control**”. McGraw- Hill, Publishing Company, New York.
- (٦٣) Snider, E. and Porter, J., (٢٠٠٢): “**Design overview-carbon adsorption**”. www.Arcesystems.com.
- (٦٤) Sawyer, C. N., and McCarthy, P. L., (١٩٧٨): “**Chemistry for Environmental Engineering**”. ٣rd Ed. McGraw-Hill, Company Inc.
- (٦٥) APHA, AWWA, APCF, (١٩٨٥): “**Standard Methods for the Examination of water and wastewater**”. ١٤th Ed. (Apha Washington, D. C.).
- (٦٦) Weber, J. W., (١٩٨٣): “**Scale up of Wastewater Treatment Process**”. Butter Worth, London.
- (٦٧) Furuya, E., Takeuchi, Y. and Noll, K. E., (١٩٨٩): “**Intraparticle diffusion of phenols within bidispersed macroreticular resin particles**”. Chem. Eng. of Japan, Vol.٢٢, No.٦, PP.٦٧٠.
- (٦٨) Sherwood, T. K., Pigford, R. L. and Wilke, C. R., (١٩٧٥): “**Mass Transfer**”. McGraw Hill. U.S.A.
- (٦٩) [Http://www.NORIT.com](http://www.NORIT.com). (٢٠٠٣): “**Measuring adsorptive capacity of powdered activated carbon**”.
- (٧٠) Abawi, S. A. and Hassan, M. S., (١٩٩٠): “**Environmental engineering water analysis**”. Al-Hikma, Al-Mosul.